New Eurasian Immigrants in the Late Paleogene of Africa, and the Great Old World Biotic Interchange: A Quantitative Analysis of Mammalian Dispersal

By Spencer Mattingly
B.Sc. Eastern Kentucky University, 2015

Submitted to the graduate degree program in Ecology and Evolutionary Biology, and the Graduate Faculty of the University of Kansas in partial fulfillment of the requirements for the degree of Doctor of Philosophy.

____

Chair: K. Christopher Beard

____

Bruce Lieberman

____

A. Townsend Peterson

____

Brian Atkinson

____

Dennis O’Rourke

Date Defended: June 8th, 2022

The dissertation committee for Spencer Mattingly certifies that this is the approved version of the following dissertation:

New Eurasian Immigrants in the Late Paleogene of Africa, and the Great Old World Biotic Interchange: A Quantitative Analysis of Mammalian Dispersal

____

Chair: K. Christopher Beard

Date Approved: June 8th, 2022

Abstract:

Following the break-up of West Gondwana in the middle Cretaceous, both Africa and South America existed in "splendid isolation", devoid of any terrestrial connections to other landmasses. This isolation led to the development of highly endemic mammal faunas on both continents. In Africa, periodic episodes of interchange occurred throughout the Paleogene, presumably via sweepstakes dispersal. These were primarily "into-Africa" invasions, with rodents and primates being among the most successful colonizers. Indeed, the late Paleogene mammal faunas of Africa are characterized by a mix of endemic afrothere taxa, and diverse assemblages of recent Eurasian immigrants. In the early Miocene, however, the Eurasian and Afro-Arabian tectonic plates collided, erasing the final vestiges of the Tethys Sea, and establishing for the first time a continuous terrestrial linkage between Africa and Eurasia. This early linkage, frequently referred to as the "*Gomphotherium* landbridge", permitted the movement of previously isolated land mammals in both directions. The resulting exchange is known as the Great Old World Biotic Interchange (GOWBI). The GOWBI is widely recognized as causing a rapid and dramatic transformation of the endemic African fauna, while having an ostensibly minimal effect on Eurasian mammals. The chapters presented herein focus on two major themes: (1) documenting new Eurasian migrants from the late Paleogene of Africa, which arrived prior to the onset of exchange in the GOWBI, and (2) measuring patterns of interchange during the GOWBI for the first time using quantitative approaches. Chapter 1 describes a new species of parapithecine primate from an early Oligocene locality in central Libya. The new species represents an intermediate form between two of the most anatomically recognizable species of stem anthropoids: *Parapithecus* and *Simonsius*. The new species, which is roughly

contemporaneous with other parapithecines from Egypt, further demonstrates habitat fragmentation and allopatric speciation in the late Paleogene of Africa. Chapter 2 details a new genus of basal carnivoraform from the same locality in Libya. The age and carnassial anatomy of the new taxon indicate that it is the first and only occurrence of a basal carnivoraform in Africa, and evidently another product of sweepstakes dispersal into Africa prior to the tectonic collision with Eurasia. Chapter 3 examines quantitative elements of diversity and evolution in the African and Eurasian faunas prior to and during the GOWBI. In doing so, it numerically documents the rapid replacement of African mammals by Eurasian immigrants, and demonstrates a pattern of asymmetry in large scale intercontinental exchange events. Together, these chapters collectively document the apparent success of Eurasian invaders in Africa both before and after the establishment of a terrestrial connection. Reasons for this success are presently unknown, but likely resulted from a combination of both biotic and abiotic factors. The GOWBI thus provide an excellent comparison for other instances of large-scale interchange in the fossil record.

Table of Contents:

Chapter 1

A new parapithecine (Primates: Anthropoidea) from the early Oligocene of Libya supports parallel evolution of large body size among parapithecids

Spencer Mattingly, K. Christopher Beard, Pauline M.C. Coster, Mustafa J. Salem, Yaowalak Chaimanee, Jean-Jacques Jaeger

Abstract:

Parapithecines are an extinct subfamily of stem anthropoid primates previously known only from the Jebel Qatrani Formation in Egypt. Here, we describe isolated teeth pertaining to *Simonsius harujensis* sp. nov., a relatively small-bodied parapithecine from strata near Zallah Oasis in the Sirt Basin of central Libya that is estimated to date to ~31 Ma on the basis of mammalian biostratigraphy. The dental morphology of *S. harujensis* sp. nov. is generally intermediate between that of the closely related parapithecines *Parapithecus fraasi* and *Simonsius grangeri*, highlighting some of the anatomical features distinguishing the latter taxa and providing further support for their generic separation. A phylogenetic analysis using parsimony methods was performed on a character-taxon matrix incorporating data from the new Libyan parapithecine, virtually all other parapithecids and the proteopithecid *Proteopithecus sylviae*. Results of this analysis suggest that parapithecids comprise a basal clade consisting of three species of *Biretia* and a more derived clade including Parapithecinae (*Parapithecus* and *Simonsius*) and Qatraniinae (*Qatrania*, *Ucayalipithecus*, and *Apidium*). Body mass estimates for parapithecids were calculated on the basis of regression equations generated to predict body mass from the occlusal area of upper and lower cheek teeth in

extant anthropoids. The relatively small body mass of *S. harujensis* sp. nov. and its reconstructed phylogenetic position as the sister group of *S. grangeri*, which is the largest known parapithecid, support the convergent acquisition of body mass larger than 500 g among multiple clades of early Oligocene African anthropoids. The new Libyan parapithecine augments previously reported evidence supporting a substantial degree of faunal provincialism across northern Africa/Arabia during the early Oligocene.

Introduction:

The Parapithecidae are a family of stem anthropoid primates with a fairly widespread distribution across Africa and the contiguous Arabian Plate during the Eocene and Oligocene (Schlosser, 1911; Simons, 1962, 1974, 1986, 1995a, 2001; Simons and Kay, 1983, 1988; de Bonis et al., 1988; Thomas et al., 1999; Simons et al., 2001; Seiffert et al., 2005; Jaeger et al., 2010; Ducrocq et al., 2011; Beard et al., 2016). In the well-documented Jebel Qatrani Formation in the Fayum region of northern Egypt, parapithecids are typically the most abundant primates and some of the most common mammals encountered at well-sampled fossil sites (Simons, 1995b). While parapithecids have been known from the later Paleogene of Africa/Arabia since the early 20th century (Osborn, 1908; Schlosser, 1911), only recently has this clade been found elsewhere. The parapithecid *Ucayalipithecus perdita* has been reported from the early Oligocene of Amazonian Peru (Seiffert et al., 2020), suggesting that two African anthropoid clades – parapithecid stem anthropoids and the crown anthropoid ancestors of platyrrhines – colonized South America at roughly the same time, presumably via sweepstakes dispersal across the South Atlantic. This pattern replicates the polyphyletic colonization of Africa by earlier anthropoids that originated in Asia (Beard, 2016).

As is the case for many other early anthropoid taxa, the phylogenetic position of parapithecids with respect to other crown and stem anthropoid clades has been contentious (Simons, 1974; Fleagle and Kay 1987; Kay et al., 2004; Seiffert et al., 2005, 2009, 2020; Beard et al., 2009; Chaimanee et al., 2012; Ni et al., 2013). Similarly, relationships within the group remain contested. Early attempts to reconstruct parapithecid phylogeny recovered a tight correlation between tree topology and either body size or stratigraphic position in the Fayum's Jebel Qatrani Formation. In other words, older and smaller taxa such as *Qatrania* were reconstructed as relatively basal parapithecids, while younger and larger parapithecids including *Apidium*, *Parapithecus*, and *Simonsius* (the latter of which has often been regarded as a junior synonym of *Parapithecus*) were reconstructed as a derived clade comprising the subfamily Parapithecinae (Kay and Williams, 1994; Ross et al., 1998; Simons et al., 2001; Seiffert et al., 2005, 2009; Seiffert, 2012). In contrast, phylogenetic analyses published by Beard and colleagues (Beard et al., 2016; Beard and Coster, 2016) recovered *Qatrania* as the sister group of *Apidium* in the subfamily Qatraniinae, while *Parapithecus* and *Simonsius* constitute the Parapithecinae. Most recently, Seiffert et al. (2020) supported the traditional content of Parapithecinae (including *Apidium*), while *Qatrania* was reconstructed as the sister group of *Ucayalipithecus*, the sole known South American parapithecid. These different tree topologies for Parapithecidae imply very different evolutionary patterns within the group, notably with respect to the duration of inferred ghost lineages and whether an increase in body size occurred once or multiple times (Beard et al., 2016).

Recent advances in our knowledge of parapithecid diversity and biogeography have focused on the smaller-bodied taxa often included in Qatraniinae (Beard et al., 2016; Beard and Coster, 2016; Seiffert et al., 2020). In contrast, undoubted parapithecines (the clade including *Parapithecus fraasi* and *Simonsius grangeri*) are currently restricted to the Fayum Depression in Egypt, and almost fifty years have elapsed since the most recently discovered parapithecine was described (Simons, 1974). Given this context, any new information on the diversity and distribution of parapithecines has the potential to illuminate broader evolutionary questions relating to parapithecids as a whole.

Here, we describe a new small-bodied parapithecine from the Sirt Basin, central Libya. The new species is only the third undoubted parapithecine to be documented to date, and it is the first verified record for this clade outside of Egypt. The new taxon, currently represented only by three isolated teeth, hails from the early Oligocene Zallah Incision local fauna (Fig. 1). The Zallah Incision local fauna was first described by Coster et al. (2015a), who advocated a biostratigraphic correlation with Fayum quarries V and G for this Libyan assemblage, making it roughly 31 Ma (Seiffert, 2006; Coster et al., 2015a). Fossil mammals documented to date from the Zallah Incision local fauna include the hystricognathous rodents *Metaphiomys zallahensis*, *Metaphiomys schaubi*, and *Neophiomys dawsonae*, the anomaluroid rodent *Prozenkerella saharaensis*, the parapithecid primate *Apidium zuetina*, the anthracothere *Bothriogenys sp*., the carnivoraform *Africtis sirtensis*, the hyracoid *Thyrohyrax libycus*, and an indeterminate sirenian (Coster et al., 2015a, 2015b; Beard et al., 2016; Mattingly et al., 2020). These taxa indicate a surprising degree of faunal provincialism across the northern margin of Africa/Arabia during the early Oligocene (Beard et al., 2017), a pattern that is made most evident by the presence of anomaluroid rodents and carnivoraforms in the Zallah Incision local fauna. Neither of these mammal clades has been documented to date from early Oligocene sites in the Fayum region of Egypt, despite a much longer history of research corresponding to a far more intensive sampling regime in the Fayum's Jebel Qatrani Formation.

Materials and methods:

Measurements and abbreviations – Standard dental measurements (Bown and Rose, 1987: Fig. 4) were obtained for the currently available sample of the new parapithecid described here and a comparative sample including other parapithecids and *Proteopithecus sylviae* using a Unitron Z binocular microscope equipped with Mitutoyo digimatic micrometers. To ensure comparability of dental metrics across taxa, measurements were taken directly from fossil specimens or high-resolution epoxy casts, with only two exceptions. In those cases, which include the holotype M_1 of *Biretia piveteaui* (BRT 17e84) and a referred M_3 of *U. perdita* (CPI 7928), dental measurements were taken from the literature (de Bonis et al., 1988; Seiffert et al., 2020).

Table 1
Digital archive and metric data (in mm) for specimens of *Simonsius harujensis* sp. nov.

Specimen	Locus	L	W	DOI
Z7I-173	left P_4	2.24	2.11	https://doi.org/10.17602/M2/M165305
Z7I-174	right M_3	3.31	2.82	https://doi.org/10.17602/M2/M165306
Z7I-175	left C_1	2.34	1.81	https://doi.org/10.17602/M2/M165307

Abbreviations – The metric abbreviations included the following: L = mesiodistal length; W = buccolingual width. The institutional abbreviations included the following: BRT = Bir el Ater collection housed at Sorbonne University (Paris, France); CGM = Egyptian Geological Museum (Cairo, Egypt); CPI = Coleccion Paleontol ogica del Insituto Geo- logico, Minero, y Metalúrgico (Lima, Peru); DPC = Division of Fossil Primates, Duke Lemur Center (Durham, North Carolina, USA); DT1 = Dur At-Talah locality 1 collection housed at University of Tripoli (Tripoli, Libya); SMNS = Staatliches Museum für Naturkunde (Stuttgart, Germany); Z7I = Zallah 7 Incision locality collection housed at University of Tripoli (Tripoli, Libya).

Phylogenetic reconstruction – A phylogenetic analysis was performed to assess the relationships of the new Libyan species with respect to other parapithecids. To do so, we updated a data matrix published by Beard and Coster (2016: Table 3), by adding three new taxa (including the new Libyan species, *U. perdita*, and *P. sylviae*) and three additional characters highlighting differences between the lower cheek teeth of *Simonsius* and *Parapithecus*. *Proteopithecus sylviae* was designated as the outgroup to Parapithecidae *sensu stricto* on the basis of its generally primitive dental morphology and a broad consensus among specialists regarding its phylogenetic position (Beard, 2002; Seiffert et al., 2005, 2020). Seven multistate characters were treated as ordered or 'additive' because they conform to natural morphoclines. A parsimony analysis of the character-taxon matrix was completed using software Tree analysis using New Technology (TNT v. 1.5; Goloboff and Catalano, 2016). A search was performed using the 'traditional search' option in TNT, with 1000 independent replications. A strict consensus tree was generated using the 'strict consensus' function in TNT. Bootstrap analyses (Felsenstein, 1985) and Bremer support indices (Bremer, 1994) were used to assess clade stability.

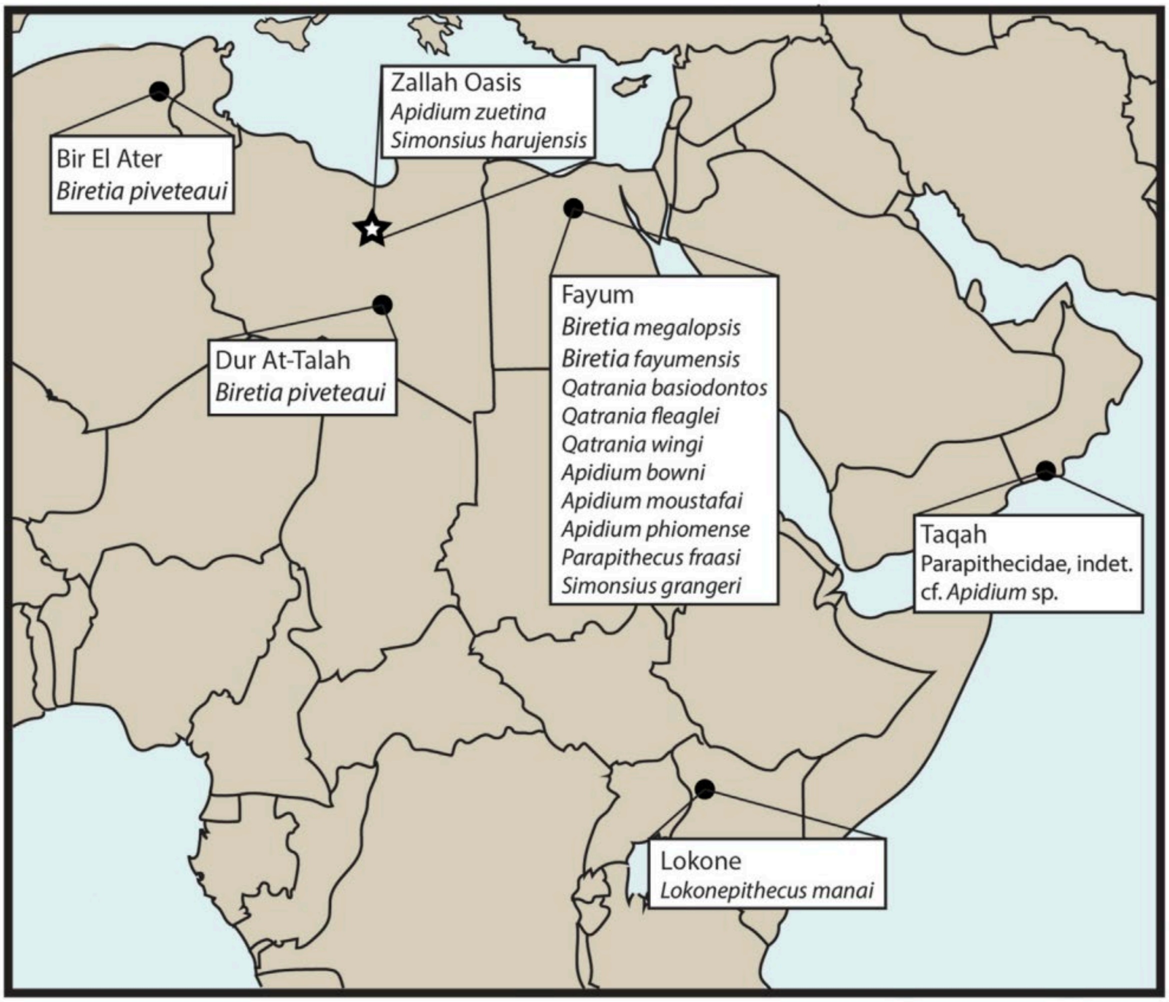

Figure 1. Documented geographic occurrences of Eocene-Oligocene Parapithecidae of Africa/Arabia.

Body mass estimates and ancestral state reconstructions – Estimates of body mass in *P. sylviae* and various species of parapithecids were obtained using regression equations calculating body mass as a function of the occlusal area of various cheek tooth loci among extant anthropoids (Egi et al., 2004: Table 2). This approach enabled us to generate multiple estimates of body mass for those fossil species that are documented by multiple tooth loci, thus mitigating potential problems related to differential scaling of individual tooth loci with respect to body mass. Differential scaling of lower molar loci with respect to body mass is pertinent in the case of parapithecids because M_3 is known to be larger relative to M_1 in *Apidium* than in *Qatrania*, for example, (Simons, 1995a). A second benefit of this approach is that it allows estimates of body mass to be calculated for poorly documented fossil species such as the new Libyan parapithecid and *U. perdita*, for which certain tooth loci (e.g., M_1) remain unknown.

To reconstruct the evolution of body mass across parapithecid phylogeny, we assigned each terminal taxon to one of six discrete character states reflecting their estimated body mass (0 = <500 g; 1 = 500-1000 g; 2 = 1000-1500 g; 3 = 1500-2000 g; 4 = 2000-2500; 5 = >2500 g). In cases where multiple estimates of body mass yielded conflicting results, we relied on estimates derived from the occlusal area of M_1 because the standard error of estimates of body mass based on this tooth locus has been shown to be lower than that of other tooth loci among extant anthropoids (Egi et al., 2004) and because M_1 has traditionally been used for this purpose among fossil primates (Conroy, 1987). M_1 remains unknown in the case of several poorly documented fossil taxa in our sample. These taxa were assigned to discrete body size character states based on estimates derived from other tooth loci and comparisons with closely related species for which M_1 is known. Treating the six body mass character states used here as an ordered or 'additive' character a posteriori, we used the 'Trace Character History' facility available in Mesquite v. 3.61 (Maddison and Maddison, 2019), to reconstruct the most parsimonious ancestral body mass at internal nodes on the strict consensus tree that we obtained for parapithecids.

Systematic paleontology

Order Primates Linnaeus, 1758

Suborder Haplorhini Pocock, 1918

Infraorder Anthropoidea Mivart, 1864

Family Parapithecidae Schlosser, 1911

Subfamily Parapithecinae Schlosser, 1911

Genus *Simonsius* Gingerich, 1978

Type species – *Simonsius grangeri* (Simons, 1974).

Included species – *Simonsius grangeri*; *Simonsius harujensis* sp. nov.

Emended diagnosis – Differs from *Parapithecus* Schlosser, 1910 in having mesiodistally reduced talonids on P_3-P_4 without a fully cuspidate hypoconid, relatively shorter and broader P_4 crown, and lower molars with more nearly distinct protocristids. M_3 differs from that of *Parapithecus* in lacking a deep, longitudinal sulcus between protoconid and metaconid; in retaining a distinct cristid obliqua; and in having the hypoconulid situated near the base of the hypoconid, rather than being separated lingually from the hypoconid by a longitudinal sulcus, thereby being positioned nearer the entoconid. *Simonsius* may also differ from *Parapithecus* in having a reduced lower adult dental formula of 0-1-3-3, although the adult lower dental formula of *Parapithecus* remains contentious.

Table 2
Dental characters selected for their phylogenetic utility among parapithecids.

Character	Character state descriptions
1	I_1: present (0); or absent (1).
2	I_2: present (0); or absent (1).
3	C_1 distolingual tubercle: absent (0); or present (1).
4	P_2 lingual cingulid: relatively linear mesiodistally (0); or deeply invaginated distally (1).
5	P_2 crown height: lower than P_3 (0); equivalent in height (1), or taller than P_3 (2)[a].
6	P_2 hypoconid: poorly developed or located well below level of P_3 trigonid (0); or elevated with respect to P_3 trigonid (1).
7	P_3 metaconid: absent (0); weak (1); or strong (2)[a].
8	P_3 postvallid crest: absent (0); or present (1).
9	P_3 talonid fovea: absent (0); or present (1).
10	P_3 hypoconid: absent or indistinct (0); present (1); or present and elevated (2)[a].
11	P_3 cristid obliqua: present, runs toward postvallid (0); present, runs toward metaconid (1); or absent/indistinct (2)[a].
12	P_4 length:width ratio: >1.10 (0); <1.10 (1).
13	P_4 talonid: small basin present (0); projects distally beyond postvallid, but without distinct basin (1); highly reduced or absent (2)[a].
14	P_4 entoconid: present (0); or absent (1).
15	P_4 cristid obliqua: present, runs toward postvallid (0); present, runs toward metaconid (1); or absent/indistinct (2)[a].
16	P_4 lingual protocristid: present (0); or absent (1).
17	P_4 hypoconid: present but weak (0); or inflated and/or elevated (1).
18	P_4 preprotocristid: trenchant (0); or weak or absent (1).
19	P_4 metaconid position on trigonid: low (0); or high (1).
20	M_1 paraconid present (0); or absent (1).
21	M_1 lingual protocristid: present (0); or absent (1).
22	M_1 centroconid absent (0); or present (1).
23	M_1 postentoconid sulcus: absent (0); or present (1).
24	M_2 paraconid: present (0); or absent (1).
25	M_2 centroconid: absent (0); present, cuspidate (1); or present, with enamel ridge invading talonid (2)[a].
26	M_2 hypoconulid: present, connected to hypoconid by postcristid or fused with its base (0); or hypoconulid present, separated from hypoconid by sulcus (1).
27	M_3 paraconid: present (0); or absent (1).
28	M_3 hypoconulid: not significantly inflated (0); or significantly inflated, projects distally beyond hypoconid (1).
29	M_3 lingual protocristid: present (0); absent, no sulcus between protoconid and metaconid (1); absent, longitudinal sulcus between protoconid and metaconid (2)[a].
30	P^2 paraconule absent (0); or present (1).
31	P^2 root number: double-rooted (0); or triple-rooted (1).
32	P^4 paraconule: absent or insignificant (0); or present and inflated (1).
33	M^1 pericone: absent (0); or present (1).
34	M^1 hypoconule: absent (0); or present (1).
35	M^2 pericone: absent or indistinct (0); or present and significantly inflated (1).
36	M^2 paraconule: present, located on preprotocrista (0); present, accompanied by dual conule located between preprotocrista and base of paracone (1); or single conule present between preprotocrista and paracone (2)[a].
37	M^2 hypoconule: absent (0); or present (1).
38	M^2 remnant of postprotocrista: present (0); or absent (1).

[a] Multistate character treated as ordered or 'additive' for purposes of parsimony analysis.

<u>Remarks</u> – The contested validity of *Simonsius* as a genus that is distinct from *Parapithecus* has been discussed extensively in the literature. The type species of *Simonsius* was originally described as *Parapithecus grangeri* Simons (1974), on the basis of its apparent affinity to the enigmatic Fayum primate *Parapithecus fraasi* Schlosser (1910). Four years later, Gingerich (1978) suggested that *Pa. fraasi*, the type locality and precise age of which remain unknown, is a junior synonym of *Apidium phiomense* Osborn (1908), which is well documented from quarries I and M in the upper part of the Jebel Qatrani Formation in the Fayum (Simons,

1995b). This left the genus *Parapithecus* (the type species of which is *Pa. fraasi*) as a junior synonym of *Apidium* Osborn, 1908, forcing Gingerich (1978) to propose the new genus *Simonsius* Gingerich, 1978 to accommodate *Pa. grangeri*. To our knowledge, subsequent workers have uniformly rejected Gingerich's (1978) proposal that *Pa. fraasi* is a junior synonym of *A. phiomense* (Kay and Simons, 1983; Fleagle and Kay, 1987; Simons and Rasmussen, 1991; Kay and Williams, 1994; Seiffert, 2012; Beard et al., 2016). However, opinions have varied as to whether *Pa. grangeri* should be retained in *Parapithecus* or sequestered in *Simonsius* (e.g., Simons, 2001; Kay et al., 2004; Beard et al., 2016; Seiffert et al., 2020). We regard this species as sufficiently autapomorphic to warrant classification in a genus distinct from *Parapithecus* (i.e., *S. grangeri*). The following description of a new and apparently more primitive species of *Simonsius* from the early Oligocene of Libya supports this interpretation.

Simonsius harujensis sp. nov. (Fig. 2)

<u>Holotype</u> – Z7I-173, left P_4 (Fig. 2A-C).

<u>Paratypes</u> – Z7I-174, right M_3 (Fig. 2D-F); Z7I-175, left C_1 (Fig. 2G-J).

<u>Type locality</u> – Zallah 7 Incision locality, Sirt Basin, Libya.

<u>Age and distribution</u> – Early Oligocene (~31 Ma) of the Sirt Basin, central Libya.

<u>Etymology</u> – Named for Jabal Al Haruj, the largest volcanic field in Libya. Late Neogene basalt flows related to the Al Haruj volcanics locally cap the early Oligocene 'Continental and Transitional Marine' stratigraphic sequence that produced these fossils (Coster et al., 2015a).

<u>Diagnosis</u> – Differs from *S. grangeri* in the following features: smaller size; C_1 smaller in relation

to P_4; talonid on P_4 less reduced but still vestigial; P_4 metaconid greatly reduced or absent; P_4 smaller in relation to M_3; and talonid of M_3 substantially narrower than trigonid.

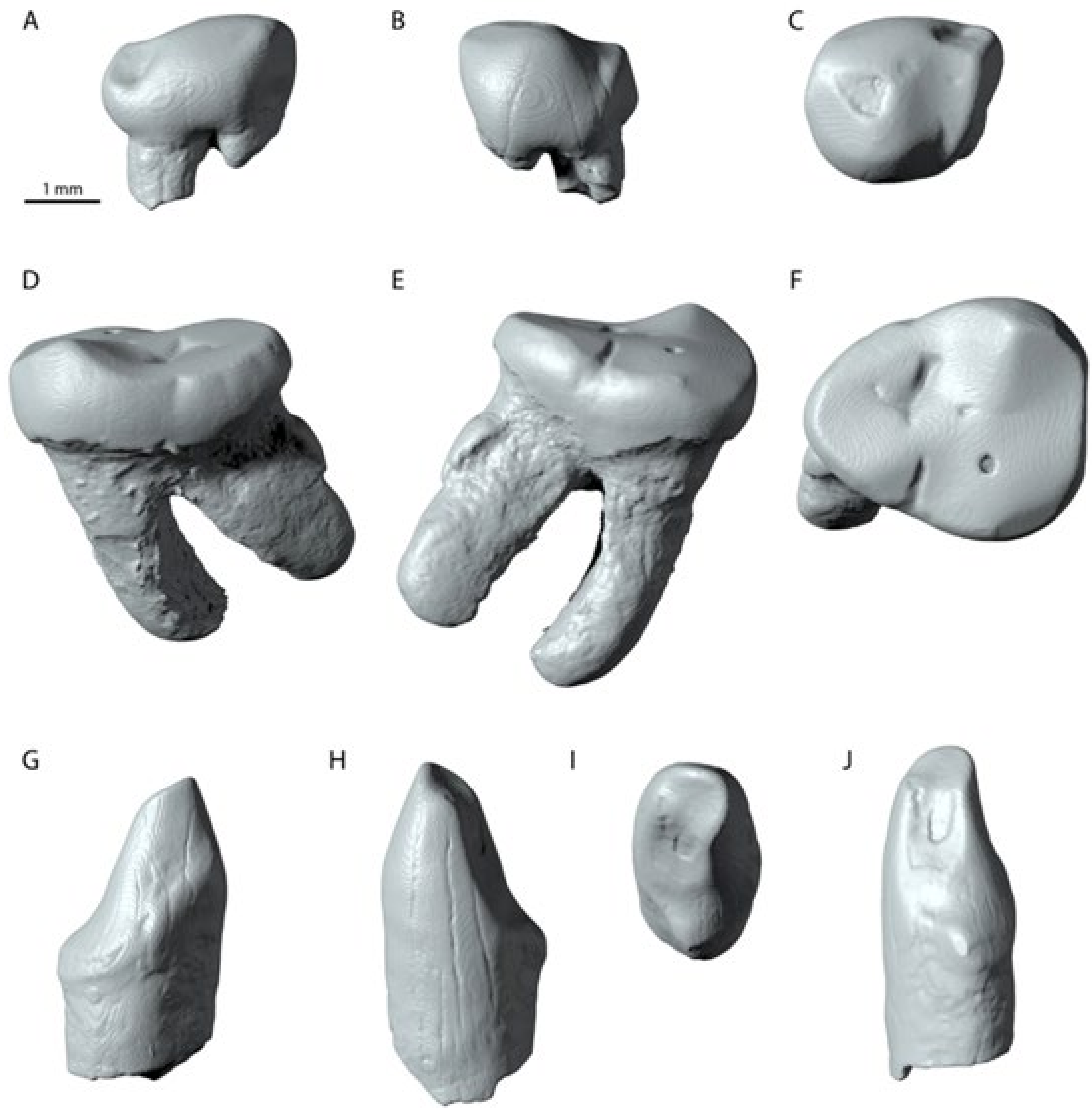

Figure 2. Isolated teeth of *Simonsius harujensis* sp. nov. from the early Oligocene Zallah Incision local fauna in the Sirt Basin, central Libya: (A–C) left P_4 (Z7I-173, holotype) in lingual (A), buccal (B), and occlusal (C) views; (D-F) Right M_3 (Z7I-174) in lingual (D), buccal (E) and occlusal (F) views; (G-J) left C_1 (Z7I-175) in lingual (G), buccal (H), occlusal (I), and distal (J) views.

Description and comparisons – Simonsius harujensis sp. nov. differs most obviously from *S. grangeri* in being considerably smaller. Currently available teeth of *S. harujensis* sp. nov. are compared with relatively complete lower dentitions of *S. grangeri* in Figure 3.

A left C_1 (Z7I-175) is attributed to *S. harujensis* sp. nov. on the basis of its small size, heavy apical wear, and morphology (Fig. 2G-J; Table 1). The crown is fairly gracile in its construction. Its apex is beveled, indicating repetitive wear with hard and/or resistant food objects, while a distal wear facet reflects shearing with the upper canine. Similar apical wear of the lower canine is relatively rare among stem anthropoids, although it occurs in some specimens of *S. grangeri* (Kay and Williams, 1994: Fig. 16c) and amphipithecid anthropoids such as *Ganlea megacanina* Beard et al. (2009) from the late middle Eocene of Myanmar. Minor abrasion of the crown makes it ambiguous whether a small interstitial wear facet may have been present on the mesial side of the C_1 crown, just above the level of the lingual cingulid, which would have been homologous with the facet that occurs at a similar location on C_1 in *S. grangeri* (Simons, 1986: Fig. 2). In *S. grangeri*, this mesial interstitial wear facet on C_1 is interpreted to reflect contact with the contralateral C_1 and the loss of both adult lower incisor loci (Kay and Simons, 1983; Simons, 1986). Given the nature of the available hypodigm for *S. harujensis* sp. nov., we refrain from making interpretations about the adult lower dental formula in this species. The base of the C_1 crown in *S. harujensis* sp. nov. is asymmetrical because of the presence of a small distolingual tubercle or cuspule, which occurs immediately lingual to the concave interstitial facet for P_2. From this cuspule, a faint lingual cingulid arises, which extends mesially and superiorly before terminating on the mesial surface below the apex. The base of the C_1 crown is similarly asymmetrical in *S. grangeri* (Kay and Williams, 1994: Fig. 16c), although the basal cuspule that is evident in Z7I-175 is less pronounced. In contrast, the base of the C_1 crown is more symmetrical in the holotype and only known specimen of *Pa.*

fraasi (Kay and Williams, 1994: Fig. 15a) and specimens of *A. phiomense* (Beard et al., 2016: Fig. 3).

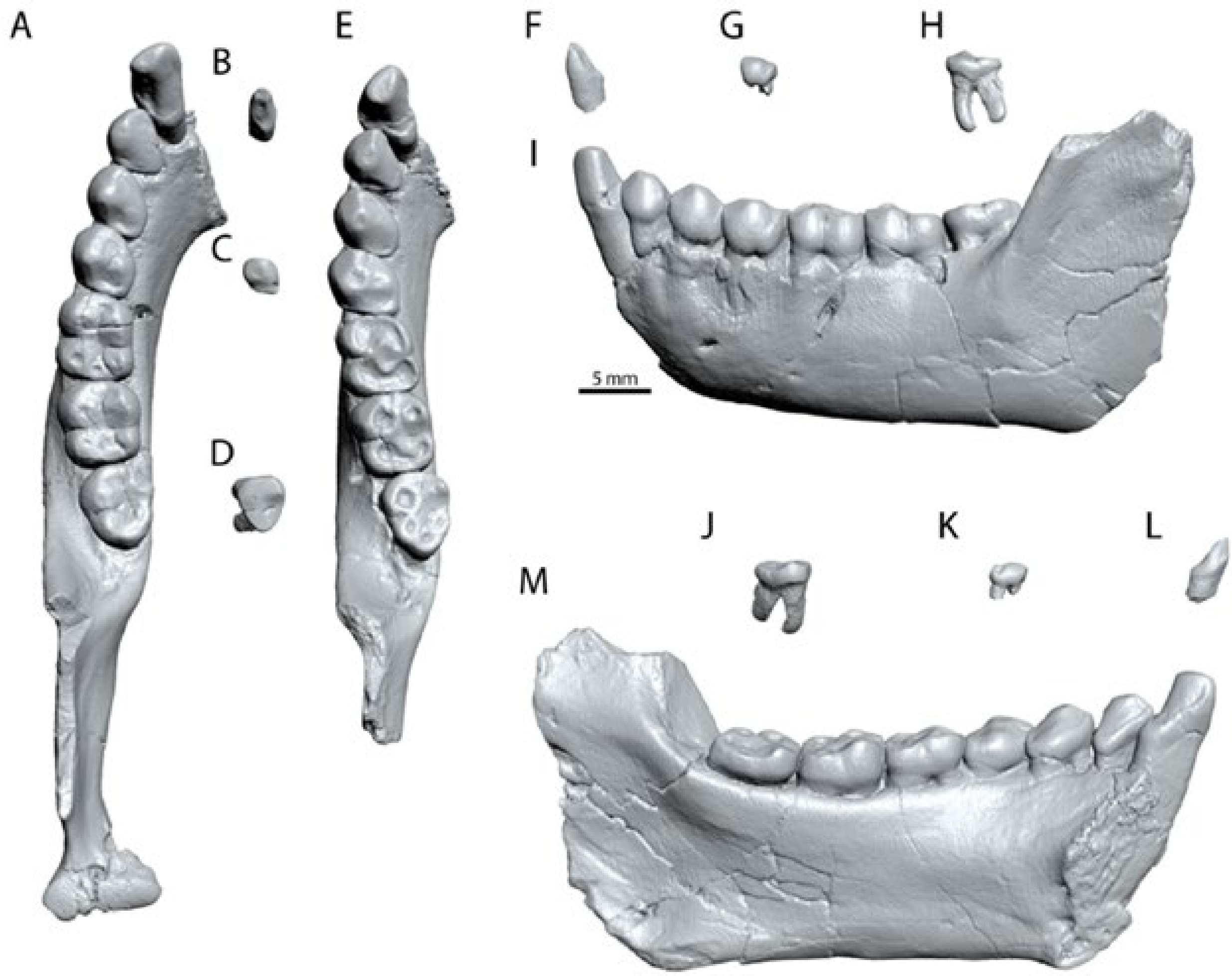

Figure 3. Lower dentitions of *Simonsius grangeri* from the early Oligocene Jebel Qatrani Formation, Fayum Depression, Egypt, compared with specimens of S. harujensis sp. nov. from the early Oligocene Zallah Incision local fauna in the Sirt Basin, central Libya. (A) Right dentary of S. grangeri (DPC 5527) preserving relatively unworn C_1–M_3 in occlusal view (reversed for comparison). (B, F, L) Left C_1 of S. harujensis sp. nov. (Z7I-175) in occlusal (B), buccal (F), and lingual (L) views. (C, G, K) Left P_4 of S. harujensis sp. nov. (Z7I-173, holotype) in occlusal (C), buccal (G), and lingual (K) views. (D, H, J) Right M_3 of S. harujensis sp. nov. (Z7I-174) in occlusal (D), buccal (H), and lingual (J) views (reversed for comparison). (E, I, M) Left dentary of S. grangeri (DPC 2807) preserving relatively worn C_1–M_3 in occlusal (E), buccal (I), and lingual (M) views.

The holotype left P_4 (Z7I-173) is a relatively low-crowned, bunodont tooth (Fig. 2A-C; Table 1). The primary cusps and crests are worn, enhancing the generally rounded nature of the crown, but these structures likely would not have been very prominent, even in an unworn condition. The trigonid is significantly inflated, particularly along its mesiobuccal margin. The protoconid is the only clearly discernible cusp, and its apex is marked by a small island of exposed dentin on the buccal side of the trigonid's occlusal surface. A mesial crest from the protoconid (paracristid or preprotocristid) is either absent or very weakly developed, in contrast to the condition in *S. grangeri*, in which such a crest is modestly trenchant and often lingually continuous with an elevated fold of enamel where a paraconid would be expected to occur. A second, much smaller island of exposed dentin is located distolingual to the apex of the protoconid. The size and position of this dentin island suggest that it marks the location of the metaconid. If so, the P_4 metaconid would have been smaller, less cuspidate and located nearer the base of the protoconid and farther distally on the trigonid than its counterpart in *S. grangeri*. A mesiodistally short, asymmetrical talonid protrudes from the distal end of the trigonid, but it lacks both a cuspidate hypoconid and a distinct cristid obliqua. A tiny island of exposed dentin may correspond to the position of a vestigial hypoconid. The abbreviation of the talonid and the inflated character of the P_4 crown have eradicated the hypoflexid. Similarly, there is no development of a talonid basin on P_4. Rather, the lingual side of the talonid is marked by a mesiodistally short, arcuate cingulid. Two roots are present, although both are broken inferiorly. They are arranged obliquely, with the mesial root being located farther buccally with respect to the larger distal root. Small interstitial wear facets on the mesiolingual and distal margins of the crown confirm that P_4 was oriented obliquely with respect to the long axis of the lower tooth row, as is typical for parapithecids and other stem anthropoids (Beard, 2002).

The only lower molar of *S. harujensis* sp. nov. currently known, Z7I-174, is a right M_3 (Fig. 2D-F; Table 1). The specimen is low crowned and bunodont, and the cusps are moderately worn, complicating efforts to interpret certain aspects of occlusal morphology. The occlusal outline of Z7I-174 is roughly triangular, with a broad trigonid and narrow talonid that tapers evenly into the hypoconulid lobe. In contrast, the occlusal outline of M_3 is more nearly rectangular in *S. grangeri* and *Pa. fraasi* because there is less disparity in the width of the trigonid and talonid in these taxa. There is little difference in height between the trigonid and talonid in Z7I-174, in which occlusal relief gradually declines from its mesial to its distal margins. The trigonid lacks any trace of either a paraconid or a paracristid. The metaconid is the most prominent trigonid cusp, occurring at the lingual terminus of a modestly elevated protocristid. Near the midline of the trigonid, the protocristid becomes indiscernible, but an island of exposed dentin farther buccally marks the location of the apex of the protoconid, which is not evident as a distinct cusp because of the moderate occlusal wear noted earlier. M_3 trigonid morphology of Z7I-174 resembles that of *S. grangeri* and differs from that of *Pa. fraasi* in retaining a relatively elevated protocristid and in lacking the longitudinal sulcus that segregates the metaconid from the protoconid in the latter taxon. Despite moderate wear, the major features of talonid morphology are recognizable in Z7I-174. A short but distinct cristid obliqua is present, located immediately lingual to a transversely oriented valley that comprises the highly abbreviated hypoflexid. In retaining a distinct cristid obliqua*, S. harujensis* sp. nov. resembles *S. grangeri* and differs from *Pa. fraasi*, in which the transversely oriented valley forming the hypoflexid continues lingually to the talonid basin, thereby obliterating the cristid obliqua. Three talonid cusps are present in Z7I-174, including a relatively large and inflated hypoconid, which is located at the distal end of the cristid obliqua near the distobuccal margin of the tooth. The much smaller and less distinctly cuspidate hypoconulid and entoconid are connected to the hypoconid by remnants of the postcristid, rather than being segregated from one another by valleys, as is the case in *Pa. fraasi*. The hypoconulid lies near the distal end of M_3 and is located near the base of the hypoconid, as is the case in *S. grangeri*, rather than being located farther lingually and more closely associated with the entoconid, which is the pattern seen in *Pa. fraasi*. M_3 is double rooted in *S. harujensis* sp. nov., and a broad, flat interstitial wear facet occurs on the mesial surface of the crown, indicating a large area of contact with the talonid of M_2.

Results:

Phylogenetic results – Character definitions and the character-taxon matrix used in the phylogenetic analysis are reported in Tables 2 and 3, respectively. Analysis of the matrix shown in Table 3 yielded three equally most parsimonious trees, a strict consensus of which is shown in Figure 4. Eocene species of *Biretia* are reconstructed as a basal clade of parapithecids, with no apparent resolution of their relationships with respect to one another. All known Oligocene species of parapithecids, along with late Eocene *Qatrania basiodontos*, belong to a second parapithecid clade that includes Parapithecinae (*Parapithecus* + *Simonsius*) and Qatraniinae (*Qatrania* + *Ucayalipithecus* + *Apidium*). Within Parapithecinae, *S. harujensis* sp. nov. is reconstructed as the sister taxon of *S. grangeri*, with *Pa. fraasi* falling out as the most basal parapithecine. Relationships among the qatraniines are consistent with those recovered by Beard and Coster (2016: Fig. 4B), despite the addition of several new characters and taxa.

Notably, the only known South American parapithecid, *U. perdita*, is reconstructed here as a basal qatraniine, being part of an unresolved polytomy alongside *Q. basiodontos* and *Q. wingi*.

Table 3
Character-taxon matrix used for phylogenetic analysis[a].

Species	Character states
Simonsius grangeri	1110101100212121011110110010100100 0201
Parapithecus fraasi	100010100120112111111011001 02?????????
Apidium bowni	00????1002101111111001101101211111 1011
Apidium moustafai	??0121200210111111 1P111111112111P01101
Apidium zuetina	??????21121??????????????21???111??1111
Apidium phiomense	00012121121011111 11P11112111211111111 1
Qatrania wingi	???????????011111110001P01011???11????
Qatrania basiodontos	???????????0111111110001001011?????????
Biretia fayumensis	??????01010000000000000P00P00??0000000
Biretia megalopsis	???1000101000000000000000000??0000000
Biretia piveteaui	??????????????????????000000???000000
Simonsius harujensis sp. nov.	??1?????????1212101 1???????101?????????
Ucayalipithecus perdita	??0???????????????????101111???111001
Proteopithecus sylviae	00001010001000200000?0010011???0010000

[a] Characters showing polymorphism for states '0' and '1' are designated as 'P' for formatting purposes.

Evolution of body mass in Parapithecidae – Dental metrics and body mass estimates for species of parapithecids and *P. sylviae* are reported in Table 4. As noted earlier, to map changes in body mass across our consensus tree topology for parapithecids, it was necessary to assign each species to a discrete body mass character state, typically on the basis of estimates derived from M_1 occlusal area. However, M_1 remains unknown for three taxa in our sample, including *A. zuetina*, *U. perdita*, and *S. harujensis* sp. nov. These taxa were assigned to discrete body mass character states on the basis of estimates derived from other tooth loci and comparisons with closely related species for which M_1 is known. Specifically, *A. zuetina* was assigned to character state '1' (500-1000 g) based on body mass estimates derived from its P_3 and P^4 (both of which are consistent with character state '1'), although it would be scored as character state '3'

(1500-2000 g) based on a similar estimate derived from its M^2. Comparing *A. zuetina* with the closely related *Apidium moustafai* shows that P_3 of *A. zuetina* is actually smaller than that of *A. moustafai,* for which M_1 is known and yields a body mass estimate consistent with character state '1'.

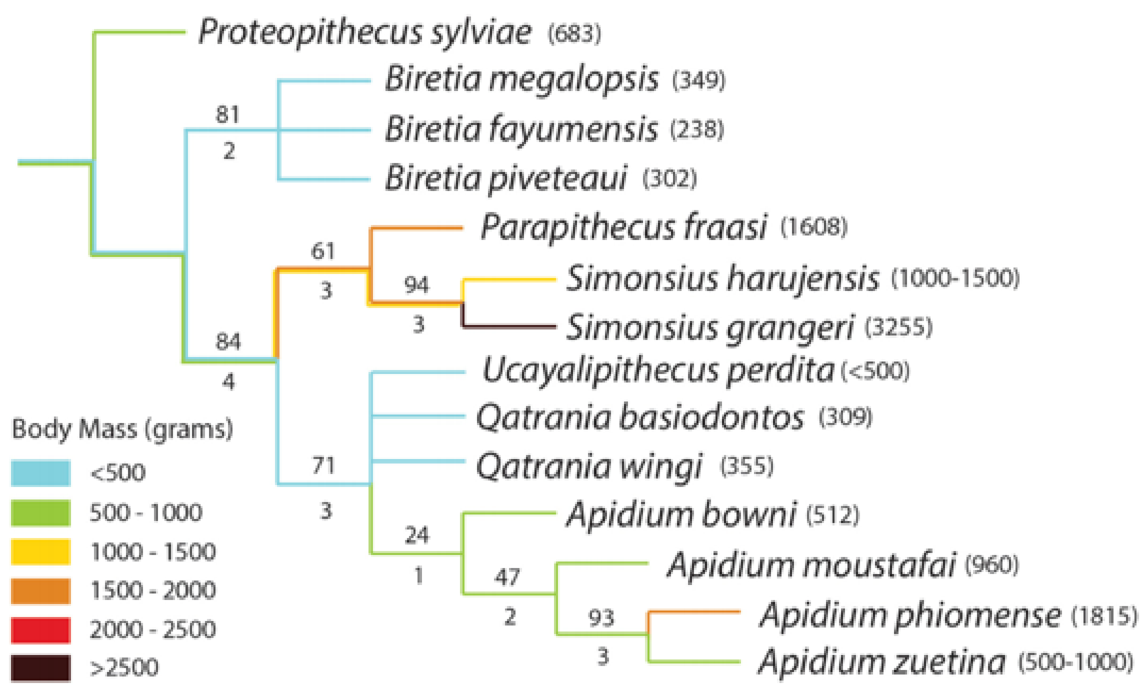

Figure 4. Strict consensus tree topology obtained from maximum parsimony analysis of the character-taxon matrix (tree length, 64 steps; consistency index, 0.734; retention index, 0.819). Bootstrap values are shown above branches. Bremer support is given below branches. Estimated body mass (g) for each terminal taxon is shown in parentheses following species name (Table 4). Ancestral state reconstructions of body mass at internal nodes are color coded to enable tracing evolution of body mass across the parapithecid tree.

Following similar logic, *U. perdita* was assigned to character state '0' (<500 g), despite the fact that its body mass as estimated on the basis of its M_3 is consistent with character state '1' (500-1000 g). Comparing *U. perdita* with the closely related *Q. wingi* shows that M_3 of *U. perdita* is actually smaller than that of *Q. wingi*, for which M_1 is known and yields a body mass estimate consistent with character state '0'. Assigning *U. perdita* to character state '0' agrees with previous estimates of the body mass of this species, which range from 319 to 366 g (Seiffert et al., 2020). Finally, *S. harujensis* sp. nov. was conservatively assigned to character state '2' (1000-1500 g). Its body mass as estimated on the basis of its P_4 is consistent with character state '1' (500-1000 g), while its body mass as estimated on the basis of its M_3 is consistent with character state '3' (1500-2000 g). Comparing *S. harujensis* sp. nov. with the closely related *Pa. fraasi* shows that its P_4 and M_3 are both substantially smaller than their counterparts in *Pa. fraasi*, for which M_1 yields a body mass estimate consistent with character state '3'.

Simonsius harujensis sp. nov., with a reconstructed body mass of 1000-1500 g, is the smallest known member of the Parapithecinae (Table 4; Fig. 4). The oldest and phylogenetically most basal members of Parapithecidae are species of *Biretia*, which are uniformly <500g in estimated body mass. Certain younger and more derived parapithecids achieved substantially larger body mass, but Beard et al. (2016) noted that large-bodied qatraniines such as *A. phiomense* and large-bodied parapithecines such as *S. grangeri* must have gotten bigger as the result of parallel evolution. The relatively small size of *S. harujensis* sp. nov. corroborates this view while also suggesting that larger body mass likely evolved in parallel even within the parapithecine clade (Fig. 4). Given that basal parapithecids (*Biretia* spp.) and basal qatraniines (species of *Qatrania* and *Ucayalipithecus*) were uniformly small (<500g), the last common ancestor of known parapithecines was probably no larger than *S. harujensis* sp. nov. If so, basal parapithecines were smaller than either *Pa. fraasi* or *S. grangeri*. A less likely but equally parsimonious alternative is that the last common ancestor of known parapithecines was the same size as *Pa. fraasi*, but this implies that *S. harujensis* sp. nov. is a phyletic dwarf. We favor the parallel evolution of larger body mass within the Parapithecinae because it reflects a broader pattern of convergent acquisition of large body mass among African anthropoids during the late Eocene and early Oligocene (Jaeger et al., 2010; Beard et al., 2016).

Table 4
Dental metric data[a] (in mm) and BM estimates[b] (in g) derived from occlusal areas of selected upper and lower cheek teeth in parapithecids and *Proteopithecus sylviae*.

Taxon	Specimen(s)	Locus	*n*	L	W	BM	BM character state[c]
Proteopithecus sylviae	CGM 42209	P_3	1	1.87	1.47	285	0
Proteopithecus sylviae	CGM 42209	P_4	1	2.03	2.00	407	0
Proteopithecus sylviae	CGM 42209, DPC 13615	M_1	2	2.90	2.72	683	1
Proteopithecus sylviae	DPC 13615	M_3	1	2.88	2.06	974	1
Proteopithecus sylviae	DPC 17372	P^4	1	2.28	3.43	774	1
Proteopithecus sylviae	CGM 41886	M^2	1	2.69	4.04	1057	2
Biretia megalopsis	DPC 21539B	P_3	1	1.94	1.68	357	0
Biretia megalopsis	DPC 21539B	P_4	1	2.13	1.79	367	0
Biretia megalopsis	DPC 22442G	M_1	1	2.68	1.94	349	0
Biretia megalopsis	CGM 83661	M_3	1	2.29	1.75	656	1
Biretia megalopsis	DPC 22279D	P^4	1	2.07	2.93	496	0
Biretia megalopsis	DPC 21358F	M^2	1	2.38	3.42	722	1
Biretia fayumensis	DPC 21296D	P_3	1	1.75	1.45	257	0
Biretia fayumensis	DPC 21757D	P_4	1	1.93	1.56	250	0
Biretia fayumensis	DPC 21220A	M_1	1	2.34	1.75	238	0
Biretia fayumensis	DPC 21371A	P^4	1	1.87	2.66	350	0
Biretia fayumensis	DPC 21539E	M^2	1	2.16	3.13	565	1
Biretia piveteaui	BRT 17-84	M_1	1	2.50	1.90	302	0
Biretia piveteaui	DT1-29	M_3	1	2.49	1.65	673	1
Biretia piveteaui	DT1-27	M^2	1	2.50	3.68	849	1
Parapithecus fraasi	SMNS 12639A	P_3	1	3.05	2.42	1043	2
Parapithecus fraasi	SMNS 12639A	P_4	1	3.17	2.68	1354	2
Parapithecus fraasi	SMNS 12639A	M_1	1	3.97	3.38	1608	3
Parapithecus fraasi	SMNS 12639A	M_3	1	4.12	3.30	2247	4
Simonsius harujensis sp. nov.	Z7I-173	P_4	1	2.24	2.11	521	1
Simonsius harujensis sp. nov.	Z7I-174	M_3	1	3.31	2.82	1538	3
Simonsius grangeri	DPC 2807, DPC 6326	P_3	2	4.03	3.58	2515	5
Simonsius grangeri	DPC 2807, DPC 6326	P_4	2	4.02	4.06	3920	5
Simonsius grangeri	DPC 2807, DPC 6326	M_1	2	4.61	4.51	3255	5
Simonsius grangeri	DPC 2807	M_3	1	5.06	3.99	3347	5
Simonsius grangeri	DPC 8793	P^4	1	3.61	6.05	4697	5
Simonsius grangeri	DPC 8793	M^2	1	4.70	5.99	3710	5
Qatrania basiodontos	CGM 42841	P_4	1	1.75	1.50	200	0
Qatrania basiodontos	CGM 42841, DPC 14236	M_1	2	2.33	2.07	309	0
Qatrania basiodontos	CGM 42841, DPC 14236	M_3	2	2.08	1.80	612	1
Qatrania wingi	DPC 6125	P_4	1	2.07	1.61	295	0
Qatrania wingi	DPC 6125	M_1	1	2.42	2.17	355	0
Qatrania wingi	DPC 6125	M_3	1	2.12	1.84	638	1
Ucayalipithecus perdita	CPI 7928	M_3	1	2.02	1.75	573	1
Apidium bowni	CGM 42199, DPC 6282	P_3	2	2.12	1.63	385	0
Apidium bowni	CGM 42199, DPC 6282	P_4	2	2.28	1.84	429	0
Apidium bowni	CGM 42199, DPC 6282	M_1	2	2.76	2.39	512	1
Apidium bowni	CGM 42199	M_3	1	2.99	2.39	1175	2
Apidium bowni	DPC 5264	P^4	1	1.99	3.57	654	1
Apidium bowni	DPC 5264	M^2	1	2.84	4.15	1177	2
Apidium moustafai	CGM 26919	P_3	1	2.59	1.88	604	1
Apidium moustafai	CGM 26919	P_4	1	2.70	2.19	751	1
Apidium moustafai	CGM 26919	M_1	1	3.43	2.84	960	1
Apidium phiomense	DPC 1102, DPC 3080	P_3	2	3.26	2.74	1340	2
Apidium phiomense	DPC 1102, DPC 3080	P_4	2	3.41	3.08	1913	3
Apidium phiomense	DPC 1102, DPC 3080	M_1	2	4.11	3.52	1815	3
Apidium phiomense	DPC 1102, DPC 3080	M_3	2	5.03	3.74	3117	5
Apidium phiomense	DPC 1048	P^4	1	3.06	5.07	2577	5
Apidium phiomense	DPC 1048	M^2	1	3.81	5.61	2580	5
Apidium zuetina	Z7I-1	P_3	1	2.38	1.91	552	1
Apidium zuetina	Z7I-4	P^4	1	1.91	3.29	528	1
Apidium zuetina	Z7I-5	M^2	1	3.41	4.46	1647	3

Abbreviations: BM = body mass; L = mesiodistal length; W = buccolingual width.
[a] Dental metrics are actual measurements (when $n = 1$) or sample means (when $n > 1$).
[b] BM estimates are derived from regression equations published by Egi et al. (2004: Table 2) that calculate BM as a function of cheek tooth occlusal area among extant anthropoids.
[c] BM character states: 0 = <500 g; 1 = 500–1000 g; 2 = 1000–1500 g; 3 = 1500–2000 g; 4 = 2000–2500 g; 5 = >2500 g.

Discussion and conclusions:

Simonsius harujensis sp. nov. possesses several characters that are hallmarks of stem anthropoid primates, including the oblique orientation of P_4 (Beard et al. 1994, 1996), the reduction or loss of the paraconid on M_3 (Fleagle and Kay, 1987; Gunnell and Miller, 2001), and the relatively small size of M_3 and its hypoconulid lobe (Fleagle and Kay, 1987). The parapithecine affinities of *S. harujensis* sp. nov. are demonstrated by its dental similarities to both *Pa. fraasi* and *S. grangeri*, several of which are highlighted in the present phylogenetic analysis. Parapithecines are united by the loss of one or more lower incisor loci, a linear P_2 lingual cingulid (as opposed to the deeply invaginated one seen in other parapithecid taxa), the absence of the M_1 lingual protocristid, and the loss of all lower molar paraconids. Within the Parapithecinae, both *S. harujensis* sp. nov. and *S. grangeri* share the presence of a distolingual tubercle on the lower canine, a smaller P_4 length:width ratio (i.e., a more compacted, inflated tooth), and the reduction or absence of the P_4 talonid. These characters support a sister group relationship between *S. harujensis* sp. nov. and *S. grangeri*, to the exclusion of *Pa. fraasi*, which retains the primitive character state in all cases.

In terms of qualitative comparisons among parapithecines, *S. harujensis* sp. nov. appears in some ways to be anatomically intermediate between *S. grangeri* and *Pa. fraasi*. In particular, P_4 in *S. harujensis* sp. nov. possesses a buccally and mesially inflated P_4 trigonid that is much larger than the reduced talonid, which bears no distinct cusps. This is in contrast to *Pa. fraasi*, which retains an inflated, cuspidate hypoconid on P_3-P_4, and shows less mesiobuccal inflation of the lower premolar trigonids. In both of these respects, the morphology of P_4 in *S. harujensis* sp. nov. more closely resembles that of *S. grangeri*, which bears extremely reduced lower premolar talonids that lack a distinctly cuspidate hypoconid. However, the distal placement and overall reduction of the P_4 metaconid in *S. harujensis* sp. nov. is more reminiscent of the condition seen in *Pa. fraasi*. P_4 in *Pa. fraasi* has a large, inferiorly and distally placed metaconid, which stands in contrast to the more mesial position of the enlarged P_4 metaconid of *S. grangeri* (Gingerich, 1978). The transverse alignment of the protoconid and metaconid on P_4 in *S. grangeri* is partly convergent on the condition seen in crown anthropoids, in which these cusps are not only aligned but joined by a transverse crest (Fleagle and Kay, 1987). Relative size comparisons between P_4 and M_3 show that *S. harujensis* sp. nov. is again intermediate between its parapithecine relatives, having a P_4 that is slightly smaller than M_3. The distal premolars of *S. grangeri* are hypertrophied to the extent that P_4 is roughly equivalent in size to M_3, while P_4 in *Pa. fraasi* is significantly smaller than M_3. While the intermediacy of *S. harujensis* sp. nov. is interesting, the derived morphology of its lower canine and P_4 warrant placement within *Simonsius* rather than *Parapithecus*. However, the fact that *S. harujensis* sp. nov. shares several dental features in common with *Pa. fraasi* suggests that the latter taxon is the best available approximation of the parapithecine dental morphotype, while the dentition of *S. grangeri* is clearly autapomorphic in many ways.

Taken together, these comparisons highlight the substantial divergence in dental morphology between *Pa. fraasi* and *S. grangeri*. Indeed, Gingerich (1978) remarked on the P4 metaconid position as evidence of a generic distinction between *Simonsius* and *Parapithecus* but stopped short of mentioning significant differences in premolar talonid morphology. Beard et al. (2016) were the first to point out differences in lower premolar morphology among parapithecines but did not include several of these characters as part of their phylogenetic analysis. The phylogenetic results presented here suggest that *Pa. fraasi* and *S. grangeri* are not as closely related as has typically been inferred, having diverged from a common ancestor that, as noted earlier, may well have been substantially smaller than either of them.

Z7I-175 is a particularly intriguing specimen of *S. harujensis* sp. nov., in that it is the only mesial tooth locus currently known for the species. Considerable research has been devoted to interpreting the lower mesial teeth and dental formulae of both *S. grangeri* and *Pa. fraasi* (e.g., Schlosser, 1911; Simons, 1974; Kay and Simons, 1983; Simons, 1986, 2001). The current consensus holds that *Pa. fraasi* retained a single pair of deciduous incisors into adulthood, while adult specimens of *S. grangeri* retained neither deciduous nor adult lower incisors (Kay and Simons, 1983; Simons, 1986). Given the fragmentary nature of the currently available sample of *S. harujensis* sp. nov. and its generally primitive morphology relative to *S. grangeri*, it remains unclear whether adult specimens of the former species possessed any lower incisors and, if so, whether they were deciduous. Simons (1986) claimed that wear facets on C_1 of *S. grangeri* made it clear that the two lower canines achieved interstitial contact in the midline. However, no such facet can be observed in Z7I-175, making similar interpretations impossible in this case.

Our demonstration of rampant parallel evolution of larger body mass among parapithecids (Fig. 4) is consistent with other studies indicating that multiple early anthropoid clades, including platyrrhines and oligopithecids, evolved from small-bodied ancestors having body mass <500g (Jaeger et al., 2010; Silvestro et al., 2019). It would not be surprising if the parallel acquisition of larger body mass among so many stem and crown anthropoid lineages coincided with mosaic evolution of discrete morphological characters and suites of characters across these taxa, promoting homoplasy during this early phase of anthropoid evolution. For example, because of well-documented shifts in dietary requirements across Kay's (1975) threshold at 500 g body mass, features that were once considered to be anthropoid synapomorphies, such as the loss of lower molar paraconids and fusion of the mandibular symphysis, may have evolved in parallel across multiple stem and crown anthropoid clades. The full extent of morphological homoplasy during early anthropoid evolution remains to be documented adequately, but it is now clear that multiple features of the anthropoid skull and dentition evolved in mosaic fashion rather than all at once, as a single integrated suite of features (Jaeger et al., 2020).

The occurrence of *S. harujensis* sp. nov. in Libya augments previous research documenting faunal provincialism among mammal faunas of northern Africa/Arabia during the early Oligocene (Coster et al., 2015a, 2015b; Beard et al., 2016, 2017; Mattingly et al., 2020). Although our knowledge of the early Oligocene Zallah Incision local fauna in the Sirt Basin of central Libya remains rather limited, it is noteworthy that both of the parapithecid primates documented from this fauna are endemic, having never been recorded from the well-known Fayum sequence in northern Egypt. Furthermore, both the Zallah Incision local fauna and contemporary faunas from the Jebel Qatrani Formation in Egypt are derived from fluviodeltaic rocks that were deposited along the southern passive margin of Tethys under similar paleoenvironmental regimes (Bown and Kraus, 1988; Swezey, 2009). Beard et al. (2016) suggested that the cooler and drier conditions of the early Oligocene may have led to greater environmental heterogeneity across the northern margin of Africa/ Arabia. These patchy environmental conditions would have disrupted gene flow over long distances, thereby promoting allopatric speciation, especially among arboreal taxa such as parapithecid anthropoids. The discovery of *S. harujensis* sp. nov. in central Libya indicates that both parapithecine and qatraniine parapithecids conform to this pattern. Further work is necessary to determine whether similar patterns of allopatric speciation prevail in propliopithecids and other North African Oligocene primate clades.

References

Beard KC. 2002. Basal anthropoids. In: Hartwig, W.C. (Ed.), The Primate Fossil Record. Cambridge University Press, Cambridge, pp. 133-149.

Beard KC, 2016. Out of Asia: anthropoid origins and the colonization of Africa. Annu. Rev. Anthropol. 45, 199e213. Beard, K.C., Coster, P.M.C., 2016. Upper molar morphology of the early Oligocene Egyptian anthropoid Qatrania wingi. Am. J. Phys. Anthropol. 159: 714-721.

Beard KC, Qi T, Dawson MR, Wang B, Li C. 1994. A diverse new primate fauna from middle Eocene fissure-fillings in southeastern China. Nature 368: 604-609.

Beard KC, Tong Y, Dawson MR, Wang J, Huang X. 1996. Earliest complete dentition of an anthropoid primate from the late middle Eocene of Shanxi Province, China. Science 272: 82-85.

Beard KC, Marivaux L, Chaimanee Y, Jaeger J-J, Marandat B, Tafforeau P, Aung Naing Soe, Soe Thura Tun, Aung Aung Kyaw. 2009. A new primate from the Eocene Pondaung Formation of Myanmar and the monophyly of Burmese amphipithecids. Proc. R. Soc. B 276: 3285-3294.

Beard KC, Coster PMC, Salem MJ, Chaimanee Y, Jaeger J-J. 2016. A new species of Apidium (Anthropoidea, Parapithecidae) from the Sirt Basin, central Libya: first record of Oligocene primates from Libya. J. Hum. Evol. 90: 29-37.

Beard KC, Coster PMC, Salem MJ, Chaimanee Y, Jaeger J-J. 2017. Biogeographic provincialism shown by Afro-Arabian mammals during the middle Cenozoic: climate change, Red Sea rifting and global eustasy. In: Agius, D.A., Khalil, E., Scerri, E.M.L., Williams, A. (Eds.), Human Interaction with the Environment in the Red Sea. Brill, Leiden, pp. 48-68.

Bown TM, Kraus MJ. 1988. Geology and paleoenvironment of the Oligocene Jebel Qatrani Formation and adjacent rocks, Fayum Depression, Egypt. US Geol. Survey Prof. Pap. 1452: 1-60.

Bown TM, Rose KD. 1987. Patterns of dental evolution in early Eocene anaptomorphine primates (Omomyidae) from the Bighorn Basin, Wyoming. Paleontol. Soc. Mem. 23: 1-162.

Bremer K. 1994. Branch support and tree stability. Cladistics 10: 295-304.

Chaimanee Y, Chavasseau O, Beard KC, Aung Aung Kyaw, Aung Naing Soe, Chit Sein, Lazzari V, Marivaux L, Marandat B, Myat Swe, Rugbumrung M, Thit Lwin, Valentin X, Zin-Maung-Maung-Thein, Jaeger J-J. 2012. Late middle Eocene primate from Myanmar and the initial anthropoid colonization of Africa. Proc. Natl. Acad. Sci. USA 109: 10293-10297.

Conroy GC. 1987. Problems of body-weight estimation in fossil primates. Int. J. Primatol. 8: 115-137.

Coster PMC, Beard KC, Salem MJ, Chaimanee Y, Brunet M, Jaeger J-J. 2015a. A new early Oligocene mammal fauna from the Sirt Basin, central Libya: biostratigraphic and paleobiogeographic implications. J. Afr. Earth Sci. 104: 43-55.

Coster PMC, Beard KC, Salem MJ, Chaimanee Y, Jaeger J-J. 2015b. New fossils from the Paleogene of central Libya illuminate the evolutionary history of endemic African anomaluroid rodents. Front. Earth Sci. 3: 56.

de Bonis L, Jaeger J-J, Coiffat B, Coiffat P-E. 1988. Decouverte du plus ancien primate catarrhinien connu dans l'Eocene sup erieur d'Afrique du Nord. C. R. Acad. Sci. Paris 306: 929-934.

Ducrocq S, Manthi FK, Lihoreau F. 2011. First record of a parapithecid primate from the Oligocene of Kenya. J. Hum. Evol. 61: 327-331.

Egi N, Takai M, Shigehara N, Tsubamoto T. 2004. Body mass estimates for Eocene eosimiid and amphipithecid primates using prosimian and anthropoid scaling models. Int. J. Primatol. 25: 211-236.

Felsenstein J. 1985. Confidence limits on phylogenies: an approach using the bootstrap. Evolution 39: 783-791.

Fleagle JG, Kay RF. 1987. The phyletic position of the Parapithecidae. J. Hum. Evol. 16: 483-532.

Gingerich PD. 1978. The Stuttgart collection of Oligocene primates from the Fayum province of Egypt. Paläontol. Z. 52: 82-92.

Goloboff PA, Catalano SA. 2016. TNT version 1.5, including a full implementation of phylogenetic morphometrics. Cladistics 32: 221-238.

Gunnell GF, Miller ER. 2001. Origin of Anthropoidea: dental evidence and recognition of early anthropoids in the fossil record, with comments on the Asian anthropoid radiation. Am. J. Phys. Anthropol. 114: 177-191.

Jaeger J-J, Beard KC, Chaimanee Y, Salem M, Benammi M, Hlal O, Coster P, Bilal AA, Duringer P, Schuster M, Valentin X, Marandat B, Marivaux L, Metais E, Hammuda O, Brunet M. 2010. Late middle Eocene epoch of Libya yields earliest known radiation of African anthropoids. Nature 467: 1095-1098.

Jaeger J-J, Sein C, Gebo DL, Chaimanee Y, Nyein MT, Oo TZ, Aung MM, Suraprasit K, Rugbumrung M, Lazzari V, Soe AN, Chavasseau O. 2020. Amphipithecine primates are stem anthropoids: cranial and postcranial evidence. Proc. R. Soc. B 287: 20202129.

Kay RF. 1975. The functional adaptations of primate molar teeth. Am. J. Phys. Anthropol. 43: 195-216.

Kay RF, Simons EL. 1983. Dental formulae and dental eruption patterns in Parapithecidae (Primates, Anthropoidea). Am. J. Phys. Anthropol. 62: 363-375.

Kay RF, Williams BA. 1994. Dental evidence for anthropoid origins. In: Fleagle, J.G., Kay, R.F. (Eds.), Anthropoid Origins. Plenum Press, New York, pp. 361-445.

Kay RF, Williams BA, Ross CF, Takai M, Shigehara N. 2004. Anthropoid origins: a phylogenetic analysis. In: Ross, C.F., Kay, R.F. (Eds.), Anthropoid Origins: New Visions. Kluwer Academic/Plenum Publishers, New York, pp. 91-135.

Linnaeus C. 1758. Systema Naturae per Regna Tria Naturae, Secundum Classes, Ordines, Genera, Species, cum Characteribus, Differentiis, Synonymis, Locies. Tomus I. Edito Decima, Reformata. Laurentii Salvii, Stockholm, p. 824.

Maddison WP, Maddison DR. 2019. Mesquite: a modular system for evolutionary analysis, Version 3.61. http://www.mesquiteproject.org.

Mattingly SG, Beard KC, Coster PMC, Salem MJ, Chaimanee Y, Jaeger J-J. 2020. A new carnivoraform from the early Oligocene of Libya: oldest known record of Carnivoramorpha in Africa. J. Afr. Earth Sci. 172: 103994.

Mivart StG. 1864. Notes on the crania and dentition of the Lemuridae. Proc. Zool. Soc. Lond. 1864: 611-648.

Ni X-J, Gebo DL, Dagosto M, Meng J, Tafforeau P, Flynn JJ, Beard KC. 2013. The oldest known primate skeleton and early haplorhine evolution. Nature 498: 60-64.

Osborn HF. 1908. New fossil mammals from the Fayûm Oligocene, Egypt. Bull. Am. Mus. Nat. Hist. 24: 265-272.

Pocock RI. 1918. On the external characters of the lemurs and of Tarsius. Proc. Zool. Soc. Lond. 1918: 19-53.

Ross C, Williams B, Kay RF. 1998. Phylogenetic analysis of anthropoid relationships. J. Hum. Evol. 35: 221-306.

Schlosser M. 1910. Über einige fossile Saugetiere aus dem Oligocän von Agypten. Zool. Anz. 35: 500-508.

Schlosser M. 1911. Beitrage zur Kenntnis der Oligozanen Land-saugetiere aus dem Fayum: Agypten. Beitrage zur Palaontol. und Geol. Osterreich-Ungarns und des € Orients 24: 51-167.

Seiffert ER. 2006. Revised age estimates for the later Paleogene mammal faunas of Egypt and Oman. Proc. Natl. Acad. Sci. USA 103: 5000-5005.

Seiffert ER. 2012. Early primate evolution in Afro-Arabia. Evol. Anthropol. 21: 239-253.

Seiffert ER, Simons EL, Clyde WC, Rossie JB, Attia Y, Bown TM, Chatrath P, Mathison ME. 2005. Basal anthropoids from Egypt and the antiquity of Africa's higher primate radiation. Science 310: 300-304.

Seiffert ER, Perry JMG, Simons EL, Boyer DM. 2009. Convergent evolution of anthropoid-like adaptations in Eocene adapiform primates. Nature 461: 1118-1121.

Seiffert ER, Tejedor MF, Fleagle JG, Novo NM, Cornejo FM, Bond M, de Vries D, Campbell Jr. KE. 2020. A parapithecid stem anthropoid of African origin in the Paleogene of South America. Science 368: 194-197.

Silvestro D, Tejedor MF, Serrano-Serrano ML, Loiseau O, Rossier V, Rolland J, Zizka A, Hohna S, Antonelli A, Salamin N. 2019. Early arrival and climatically-linked geographic expansion of New World monkeys from tiny African ancestors. Syst. Biol. 68: 78-92.

Simons EL. 1962. Two new primate species from the African Oligocene. Postilla 64: 1-12.

Simons EL. 1974. Parapithecus grangeri (Parapithecidae, Old World higher primates): new species from the Oligocene of Egypt and the initial differentiation of Cercopithecoidea. Postilla 166: 1-12.

Simons EL. 1986. Parapithecus grangeri of the African Oligocene: an archaic catarrhine without lower incisors. J. Hum. Evol. 15: 205-213.

Simons EL. 1995a. Crania of Apidium: primitive anthropoidean (Primates, Parapithecidae) from the Egyptian Oligocene. Am. Mus. Novit. 3124: 1-10.

Simons EL, 1995b. Egyptian Oligocene primates: a review. Yearbk. Phys. Anthropol. 38: 199-238.

Simons EL. 2001. The cranium of Parapithecus grangeri, an Egyptian Oligocene anthropoidean primate. Proc. Natl. Acad. Sci. USA 98: 7892-7897.

Simons EL, Kay RF. 1983. Qatrania, new basal anthropoid primate from the Fayum, Oligocene of Egypt. Nature 304: 624-626.

Simons EL, Kay RF. 1988. New material of Qatrania from Egypt with comments on the phylogenetic position of the Parapithecidae (Primates, Anthropoidea). Am. J. Primatol. 15: 337-347.

Simons EL, Rasmussen DT. 1991. The generic classification of Fayum Anthropoidea. Int. J. Primatol. 12: 163-178.

Simons EL, Seiffert ER, Chatrath PS, Attia Y, 2001. Earliest record of a parapithecid anthropoid from the Jebel Qatrani Formation, northern Egypt. Folia Primatol. 72: 316-331.

Swezey CS. 2009. Cenozoic stratigraphy of the Sahara, northern Africa. J. Afr. Earth Sci. 53: 89-121.

Thomas H, Roger J, Sen S, Pickford M, Gheerbrant E, Al-Sulaimani Z, AlBusaidi S. 1999. Oligocene and Miocene terrestrial vertebrates in the southern Arabian Peninsula (Sultanate of Oman) and their geodynamic and palaeogeographic settings. In: Whybrow, P.J., Hill, A. (Eds.), Fossil Vertebrates of Arabia. Yale University Press, New Haven, pp. 430-473.

Chapter 2

A new carnivoraform from the early Oligocene of Libya: Oldest known record of Carnivoramorpha in Africa

Spencer G. Mattingly, K. Christopher Beard, Pauline M.C. Coster, Mustafa J. Salem, Yaowalak Chaimanee, Jean-Jacques Jaeger

Abstract:

Carnivoraformes is a clade comprised of members of the Carnivora, as well as the paraphyletic assemblage of stem taxa previously united under the “Miacidae”. Here we describe the earliest known African occurrence of a carnivoraform from the early Oligocene Zallah Incision locality in the Sirt Basin of central Libya. The new taxon is represented by three teeth (M_1, P^4, and dP^3), all of which are carnassial loci diagnostic of the Carnivoraformes. Despite its meager anatomical representation, the new Libyan carnivoraform possesses numerous characters that distinguish it from contemporaneous African hyaenodonts, including the retention of a large M_1 metaconid, an enlarged and transversely oriented P^4 metastyle, and the absence of a metacone on dP^3, among other features. The generally primitive nature of known tooth loci and the absence of clear synapomorphies with crown carnivorans suggest that the new carnivoraform may be a relatively basal member of the clade. If so, the new Libyan taxon would be the only known African occurrence of a basal carnivoraform.

Introduction:

Carnivoramorpha is a clade of mammals that includes all members of Carnivora and their stem lineage, the latter of which are often united under the name “Miacoidea” (Wyss and Flynn, 1993). In its current conception, “Miacoidea” includes the basal Viverravidae and the paraphyletic assemblage of taxa historically known as the “Miacidae”. Numerous authors have remarked on the paraphyly of “miacids” and advocated for an abandonment of the term (e.g. Spaulding et al., 2010; Spaulding and Flynn, 2012). Flynn et al. (2010) erected the group Carnivoraformes to include Carnivora plus the “Miacidae”, and subsequent workers have referred to “miacids” as “basal carnivoraforms” (Solé, 2014a; Solé et al., 2014, Solé et al., 2016a). Here we follow this convention.

Carnivoramorphans are well documented from the early Paleogene of all three Laurasian continents (e.g., Fox and Youzwyshyn, 1994; Huang et al., 1999; Tong and Wang, 2006; Fox et al., 2010; Solé et al., 2016a). However, their definitive presence in Africa is restricted to the Neogene. The earliest undoubted African carnivoramorphan, *Mioprionodon hodopeus*, comes from the Nakwai locality in northwestern Kenya (Rasmussen and Gutierrez, 2009). Nakwai was originally interpreted as late Oligocene in age, based on biostratigraphic correlation of its mammalian fauna (Rasmussen and Gutierrez, 2009). More recently, the site was radiometrically dated to approximately 22 Ma (earliest Miocene), thereby eliminating the only Paleogene record of undoubted Carnivoramorpha in Africa (Rasmussen et al., 2019). However, two substantially older records of purported carnivoramorphans have been reported from the African Paleogene. Gheerbrant (1995) described a single tooth (THR 299) from the late Paleocene of the Ouarzazate Basin in Morocco, which he identified as the P^4 of a basal carnivoramorphan. Subsequently, Crochet et al. (2001) described an isolated M_1 from the late early or early middle Eocene of Algeria as the holotype of *Glibzegdouia tabelbalaensis*, which they regarded as a carnivoran (carnivoramorphan according to current usage). Werdelin and Peigné (2010) questioned the carnivoran affinities of both of these early Paleogene African fossils, noting that they might better be regarded as hyaenodonts. Solé et al. (2014b) described additional specimens of *Glibzegdouia tabelbalaensis*, which they interpreted as supporting its inclusion within the hyaenodont clade Teratodontinae. Thus, pending further study and/or the recovery of additional material pertaining to whatever taxon THR 299 represents, the oldest African fossils that can reliably be referred to Carnivoramorpha date to the early Miocene.

Even so, recent studies using molecular data have suggested a potential Oligocene presence of Carnivora in Africa. For example, Eizirik et al. (2010) found that the Eupleridae, a clade of crown carnivorans endemic to Madagascar, diverged around 25.5 Ma (late Oligocene). Given that the sister group of Malagasy Eupleridae is the African and Asian mongoose clade Herpestidae (Yoder et al., 2003; Eizirik et al., 2010; Rolland et al., 2015), it is highly likely that the common ancestor of euplerids and herpestids lived in Africa. Yoder et al. (2003) similarly estimated the divergence between Eupleridae and Herpestidae as 18–24 Ma, suggesting that the common ancestor of these clades lived in Africa during the late Oligocene or early Miocene. Rolland et al. (2015) estimated the timing and patterns of dispersal of various carnivoran groups, suggesting that members of the order likely dispersed to Africa between 30 and 20 Ma, corresponding to the closure of the Tethys sea. Taken together, these molecular data are compatible with a carnivoran presence in Africa during the late Oligocene, although the fossil record has yet to corroborate this hypothesis.

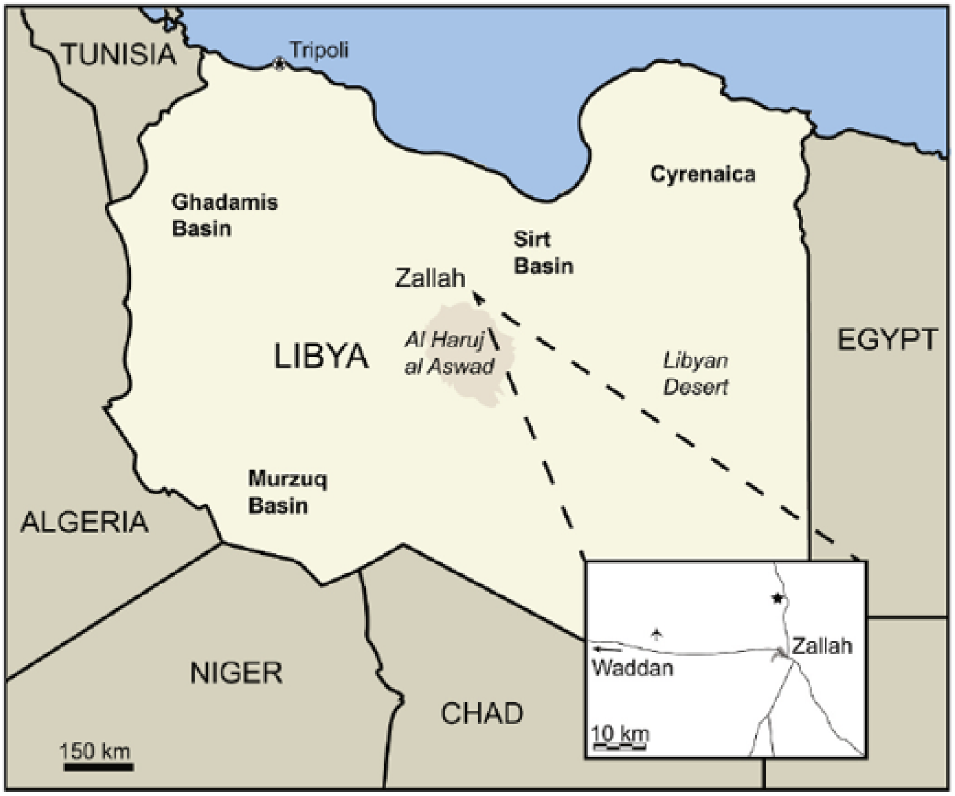

Figure 1. Map of Libya and adjacent areas showing the location of Zallah Oasis in the Sirt Basin. Inset shows the location of the Zallah 7 Incision locality (Z7I locality), denoted by a star.

Here, we report the discovery of a new carnivoraform from the Zallah Incision local fauna in the Sirt Basin of Libya (Fig. 1). The new taxon is provisionally interpreted as a basal carnivoraform because of its primitive carnassial morphology, but it is currently too poorly documented to assess its phylogenetic position within Carnivoraformes more rigorously. The Zallah Incision local fauna was first described by Coster et al. (2015a), who also discussed the history of paleontological exploration in the vicinity of Zallah Oasis as well as the local geological context. Additional fossil mammals from this local fauna, including the anomaluroid rodent *Prozenkerella saharaensis* and the parapithecid primate *Apidium zuetina*, were subsequently described by Coster et al. (2015b) and Beard et al. (2016). Biostratigraphic correlation based primarily on fossil rodents and primates suggests that the Zallah Incision local fauna is close in age to quarries V and G in the Upper Sequence of the Jebel Qatrani Formation in the Fayum Depression of northern Egypt (Coster et al., 2015a; Beard et al., 2016). Assuming that this correlation is accurate, the Zallah Incision local fauna dates to the early Oligocene or ~31 Ma (Seiffert, 2006; Coster et al., 2015a). The new taxon described here thus represents the earliest known occurrence of a carnivoramorphan in Africa. We refrain from assigning the new taxon to any particular family because of the fragmentary nature of the available material and the limited sampling of dP3 among basal carnivoraforms. Despite the limited nature of the hypodigm, the new Libyan taxon is morphologically diagnostic, enabling it to be named for ease of reference in the scientific literature.

The permanent repository for all specimens described here is the paleontological collection housed by the Geology Department of the Faculty of Science, University of Tripoli, Libya. All specimens are also accessible on Morphosource (morphosource.org), with DOI links provided below.

Systematic paleontology

Carnivoramorpha Wyss and Flynn, 1993

Carnivoraformes Flynn et al., 2010

Family *incertae sedis*

Africtis sirtensis, gen. et sp. nov.

Holotype — Z7I-11, right m1 (Fig. 2a–c; https://doi.org/ 10.17602/M2/M157609).

Etymology — The generic name combines Africa with the Latin *ictis* (weasel), a common suffix for Paleogene carnivoramorphans. The trivial name recognizes the provenance of this taxon as the Sirt Basin.

Hypodigm — Z7I-171, right P^4 (Fig. 2d–f; https://doi.org/ 10.17602/M2/M157610); Z7I-172, right dP3 (Fig. 2g–l; https://doi. org/10.17602/M2/M157611).

Type locality — Zallah 7 Incision (Z7I) locality, Sirt Basin, Libya.

Age and distribution — Early Oligocene of the Sirt Basin, central Libya.

Measurements — Table 1.

Diagnosis — Small carnivoraform differing from all other carnivoraforms in having the following combination of features: M_1 trigonid cusps short and robust; M_1 postfossid shallow and buccolingually narrow; M_1 hypoconid large and relatively mesial in position; M_1 hypoconulid lobe closely appressed to the hypoconid; lack of a continuous buccal cingulid on M_1; P^4 protocone large, bulbous, and mesiolingual in position; P^4 parastyle and parastylar root markedly reduced; distolingual cingulum on P^4 originates distally, without connection to postprotocrista; dP^3 parastyle highly reduced or absent; dP^3 metastyle extremely elongated; mesial cingulum on dP^3 present; dP^3 protocone extremely reduced; greatly reduced or absent buccal cingulum on dP^3; dP^3 paracone inclined buccally. Differs from *Mioprionodon hodopeus* in having M_1 with less trenchant carnassial crests, larger hypoconid, and basal circumference of metaconid larger in diameter. Differs from early Miocene herpestids in having M_1 with mesiodistally abbreviated talonid, distinct entoconid absent, hypoconid reduced in height, and trigonid more compact mesiodistally.

Table 1

Metric data (in mm) for specimens of *Africtis sirtensis*. Asterisks indicate incomplete measurements due to breakage or heavy cusp wear.

	m1 (total)	m1 (trigonid)	m1 (talonid)	P4	dP3
Length (mesiodistal)	4.88	3.25	1.63	3.42*	3.12
Width (buccolingual)	2.81	2.81	1.72	4.02*	2.46
Height (dorsoventral)	3.83	3.83	1.56	2.13*	1.55*

Description – The M_1 of *Africtis sirtensis* (Fig. 2a–c) is fairly low crowned and robust. The trigonid is buccolingually narrow, but considerably broader than the highly reduced talonid. The protoconid is the largest trigonid cusp, but its height does not exceed that of the paraconid by a wide margin. The preprotocristid is moderately developed though slightly convex, and it therefore does not form a perfectly straight occlusal edge. It joins the trenchant paracristid at a deep carnassial notch. The paraconid is buccolingually broad, and projects mesially at a 60 degree angle relative to the jaw. The metaconid is broken, but likely would have been well developed. Its base is broad and closely appressed to the protoconid. A thin precingulid is present on the mesiobuccal aspect of the crown. It originates just below the apex of the paraconid and extends buccally around the inferior margin of the crown, terminating below the apex of the protoconid. Mesially, it reaches a height nearly half that of the paraconid, and bears a tiny interstitial wear facet for P_4. The mesiobuccal surface of the trigonid is dominated by a large shearing facet (Fig. 3a–b). Less visible are the vertical wear striae that span the dorsoventral length of the facet. The facet occupies virtually all of the buccal surface of the paraconid, and spans the entire carnassial notch, disappearing roughly halfway across the mesiodistal length of the protoconid. It is more heavily abraded along its mesial aspect, below the paraconid. The distal wall of the trigonid or postvallid also bears a large shearing surface, which is adorned by a series of parallel, slightly-oblique wear striae that run from dorsolingual to ventrobuccal (Fig. 3c–d). These striae extend down the postvallid wall into the hypoflexid, and are oriented at an angle of roughly 20–25° from the vertical. The talonid of M_1 is reduced in size and complexity. It is compressed buccolingually, such that its width spans only two-thirds that of the trigonid. The hypoconid is the only distinct talonid cusp. It is large, however, and its height is roughly equivalent to the mesial terminus of the precingulid. The apex of the hypoconid is situated somewhat mesially, rather than being located near the distolingual margin of the talonid. Its base is greatly inflated, protruding lingually into the talonid basin. The short cristid obliqua runs forward from the hypoconid, and descends inferiorly as it approaches the postvallid. It forms a small notch near its mesial end, along with a diminutive crest originating from the postvallid. This notch is deepened by an incipient cuspule at the mesial end of the cristid obliqua. The cristid obliqua is oriented mesiodistally, and it bears a small, rectangular wear facet on its buccal surface. A small projection, ostensibly a hypoconulid lobe, extends distolingually from the hypoconid, although no distinct hypoconulid cusp is present. This projection is the distalmost point on the tooth. A prominent wear facet lies just buccal to the hypoconulid lobe, and directly distal to the hypoconid. The shape of the facet is that of an inverted triangle. The entoconid is completely absent, and the entocristid is low, but it slightly closes the postfossid lingually. The postfossid is buccolingually narrow, and dorsoventrally shallow. The large base of the hypoconid intrudes upon it buccally. There is a small, semicircular wear facet on the distal aspect of the talonid, indicating interstitial contact with a low-crowned M_2. The facet is only visible in distal view.

The P^4 of *Africtis sirtensis* (Fig. 2d–f) is heavily worn in the only example of this locus currently known. The paracone is the largest cusp, although its distobuccal border is broken. The base of the cusp is large and slightly distally inclined as it tapers toward its apex. The preparacrista is very weakly developed, to the point that it is nearly absent. There is no basin separating the paracone from the protocone. Rather, the protocone nearly merges with the base of the paracone, separated only by a small furrow. Within this furrow exist two small, but noticeable wear facets: one mesiobuccal to the protocone, and one distobuccal (Fig. 3f). Both facets are shallow depressions that slightly disturb the otherwise smooth outline of the protocone/paracone furrow. The mesial facet is more deeply excavated, and more rounded in shape. The distal facet is flatter and shallower, and slightly extends onto the distal base of the paracone. The protocone itself is a large, bulbous cusp that is located mesiolingual to the paracone, although its unworn apex may have been located farther mesially, due to the distal inclination of the paracone. The parastylar lobe is poorly developed, and the parastyle itself is notably absent. A buccal cingulum is continuous with the parastylar lobe, and is oriented distobuccally prior to its break below the paracone. There is no mesial cingulum. A distal cingulum is present, but this structure is not continuous with a postprotocrista, which is absent. The distal cingulum arises distal to the paracone and is angled distobuccally. The metastyle is broken, but likely would have extended distobuccally. The distobuccal root, which supports the mestastyle, is displaced buccally, such that it is not in line with the mesiobuccal root, which is highly reduced. The lingual root, supporting the protocone, is large and inclined lingually.

The dP^3 of *Africtis sirtensis* (Fig. 2g–i) is considerably smaller than P^4 in all dimensions, most notably buccolingual width. The cusps and crests of dP^3, including the metastylar blade, are heavily worn. The base of the crown is open, bearing no remnant of the roots. Together with the substantial wear noted previously, the resorption of the roots indicates that Z7I-172 represents an older juvenile individual in which dP^3 was about to be shed. The paracone is by far the largest cusp. It is buccally inclined. The preparacrista is moderately developed, and extends mesially to contact the small mesial cingulum. No parastyle or parastylar lobe is present, although there is a small break at the mesiobuccal margin of the crown, indicating that a vestigial parastylar lobe may have existed. The mesial cingulum is thin and apparently continuous with the preprotocrista. The protocone itself is little more than a broad, lingually flattened wear facet; no cusp formation is evident. The protocone does not project far lingually, giving the entire tooth a narrow, vaguely L-shaped appearance. The protocone is not separated from the paracone by a distinct basin. No postprotocrista is apparent. A small distal cingulum arises from the distal base of the paracone and terminates at the distal end of the metastyle. The metastyle is elongated and oriented distobuccally. There is little buccal expansion, however, relative to that presumed in P^4 (Z7I-171). The mesial margin of the metastyle joins the postparacrista at a relatively shallow carnassial notch. The postparacrista is angled distolingually. There is no buccal cingulum.

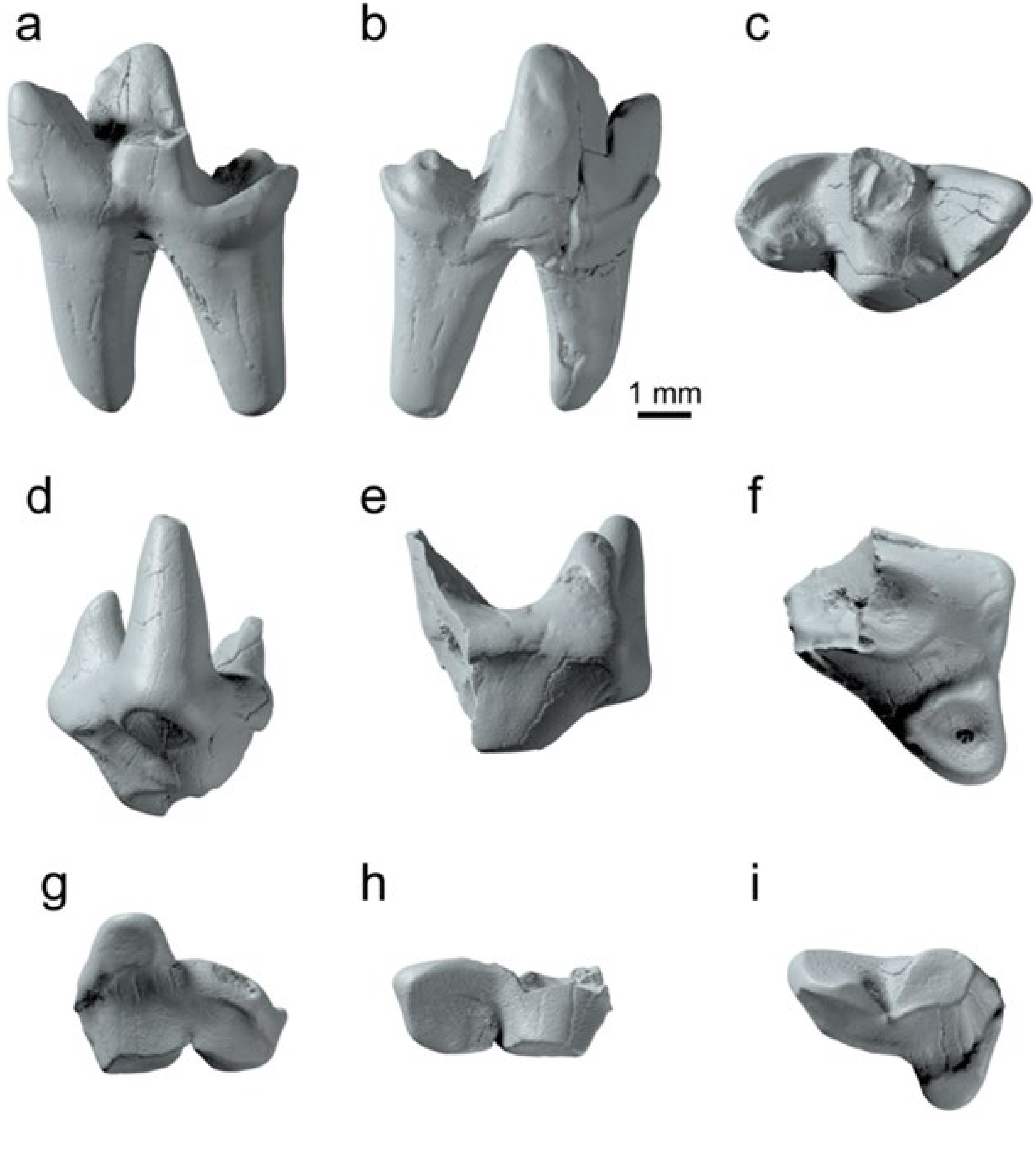

Figure 2. Isolated teeth of *Africtis sirtensis*, gen. et sp. nov., from the early Oligocene Zallah Incision local fauna in the Sirt Basin, central Libya. (a-c) holotype right M_1 (Z7I-11) in lingual (a), buccal (b), and occlusal (c) views. (d-f) right P^4 (Z7I-171) in lingual (d), buccal (e), and occlusal (f) views. (g-i) right dP^3 (Z7I-172) in lingual (g), buccal (h), and occlusal (i) views.

Remarks:

Conspecificity – All three specimens assigned to *Africtis sirtensis* are interpreted as conspecific for the following reasons: P^4 and M_1 match very closely in size; dP^3 is compatible in size with both P^4 and M_1, particularly in mesiodistal length, but it is narrower and shorter in terms of crown height, as would be expected for deciduous premolars (Zack, 2012); P^4 and dP^3 share a reduction of the parastyle; P^4 and dP^3 share a reduced (virtually absent) trigon basin between the paracone and protocone; M_1 and P^4 share an overall "mesocarnivorous" morphology, considering the size and presence of their major cusps, as well as the poor development of their shearing crests; and all three tooth loci separately exhibit characters that resemble conditions found in basal Laurasian carnivoraforms. Finally, parsimony suggests that these isolated teeth pertain to a single carnivoraform taxon, especially considering that no other carnivoraform is definitively known from the African Paleogene.

The identification of Z7I-171 as a permanent tooth requires further discussion, given some unusual aspects of its morphology. Most notably, its mesiobuccal root, which supports the parastyle, is highly reduced (Fig. 2e). Frequently, such a gracile root morphology is characteristic of deciduous teeth, as their roots are gradually resorbed in response to the development and eruption of the associated permanent tooth locus (Mellet, 1977). Further, the roots of Z7I-171 are widely splayed, which is another hallmark of deciduous teeth (Fox and Youzwyshyn, 1994). The protocone root, for instance, slants lingually, such that its apex extends lingually beyond the crown margin. The metastylar root is similarly splayed distobuccally. Lastly, the protocone is located farther distally than is typical in both "creodonts" and carnivorans, in which the P^4 protocone nearly always lies in advance of the paracone. A more distally situated protocone is often observed in dP^3, however (Butler, 1946; Fox and Youzwyshyn, 1994). Despite these unusual characters that mimic conditions seen in dP^3, Z7I-171 is interpreted as a P^4 on the basis of the size and shape of its protocone. The large, bulbous protocone morphology found in Z7I-171 is more characteristic of an adult P^4, because this cusp is often reduced in dP^3 among carnivoramorphans (Fox and Youzwyshyn, 1994). Identification of Z7I-171 as a P^4 is further corroborated by the buccal expansion of its metastyle, which does not occur in deciduous carnassials, the occlusal outlines of which are notably “T-shaped” (Fox and Youzwyshyn, 1994).

The perceived buccal expansion of the P^4 metastyle is critical to the designation of *Africtis sirtensis* as a carnivoraform and not a hyainailouroid. Despite breakage of the crown distal to the paracone (Fig. 2f), significant buccal expansion is inferred based on three lines of evidence: (1) the distobuccal angling of the break itself makes it clear that the metastyle would have continued in this direction if it were preserved; (2) the distobuccal orientation of both the buccal and distal cingula - which collectively envelop the metastyle - prior to their breakage implies that these cingula, and thus the metastyle itself, would have extended distobuccally; and (3) the buccal position of the distobuccal root, which supports the metastyle. Although the root itself is broken, that which remains of the root makes it clear that this structure would have been implanted in the maxilla more buccally than the parastyle, paracone, and mesiobuccal root. The buccal position of the distobuccal root implies that the metastyle would have been similarly oriented relative to the longitudinal axis of the tooth.

Identification of dP3 – Z7I-172 (Fig. 2g–i) is clearly a deciduous tooth based on several characteristics, the most obvious of which are the absence of any roots and the open base of the crown. These two features virtually reduce the specimen to a hollow shell of enamel, lacking much of its dentin core. Its deciduous nature is further evidenced by the diminutive size of the protocone, the central position of the protocone relative to the paracone, and the mesiodistally elongate and buccolingually narrow occlusal outline of the crown (Butler, 1952; Fox and Youzwyshyn, 1994; Zack, 2012). The small size of the protocone is unlikely to be due to wear, given the veritable flatness of its surface. The large size of the metastyle and the highly reduced protocone are the most interesting features of Z7I-172, indicating a highly secant deciduous dentition. This contrasts somewhat with the morphology of permanent P^4 and M_1, both of which display more mesocarnivorous characteristics.

Wear facets – The presence of various wear facets on M_1 imply some information about the upper dentition, including P^4 and M^1, in *Africtis sirtensis*. Most notably, the expansive shearing facet on the mesiobuccal trigonid of M_1 (Fig. 3b) suggests a fair degree of occlusion with the metastyle of P^4. The relatively weak development of the wear striae, however, indicates that the P^4 metastyle, which is broken in Z7I-171, was likely not hypercarnivorous or fully trenchant. Nonetheless, this specialized occlusion between P^4 and M_1 is a hallmark of Carnivoramorpha, in contrast to the more distally located postvallum/prevallid shear of “creodonts” (Fox et al., 2010). Further, the oblique striae along the postvallid of M_1 (Fig. 3c–d) add additional evidence for the carnivoran affinities of *Africtis sirtensis*. This prevallum/postvallid shear between M^1 and M_1, respectively, may distinguish Carnivora from other Paleogene carnivorous mammals (Fox and Youzwyshyn, 1994; Fox et al., 2010). Specifically, this refers to occlusion between the mesial-most aspects of M^1 (e. g. the parastyle, preparacrista, preprotocrista, etc.) and the distal trigonid wall of M_1. This differs from the postvallum/prevallid shear that dominates "creodont" molars (Solé et al., 2009; Fox et al., 2010). Further, both the small size of the cristid obliqua on M_1 and the inconspicuous shearing facet it bears buccally indicate poor development of the postparacrista on M^1. The paracone itself was likely large, however, given the diminutive size of the M_1 ectocingulid (Solé et al., 2009). The metacone was likely well-separated from the paracone, based on the prominent shearing facet it left just distal to the apex of the M_1 hypoconid. Its height was probably less than that of the paracone, given that the metacone's occlusal facet does not extend as far down the crown of M_1. The protocone, by contrast, is inferred to be comparatively small, due to the shallow depth and narrow dimensions of the M_1 talonid.

Similarly, two distinct wear facets on Z7I-171 allow inferences about the postvallid morphology of P_4. These wear facets, which appear as shallow fossae between the P^4 paracone and protocone (Fig. 3e–f), likely exist as a result of contact between P^4 and two posterior accessory cusps on the buccal margin of P_4. The mesial facet, which is more deeply excavated, shows that the first posterior accessory cusp on P_4 was likely the larger of the two, and possessed little capacity for shearing. The distal facet, by contrast, is a flatter, shallower excavation that suggests some shearing function of the second posterior accessory cusp on P_4. These cusps, in combination with an elongated talonid, comprise the elaborate P_4 postvallid that is diagnostic of the order Carnivora (Flynn and Galiano, 1982; Gheerbrant, 1995), although their presence in *Africtis sirtensis* can only be inferred here.

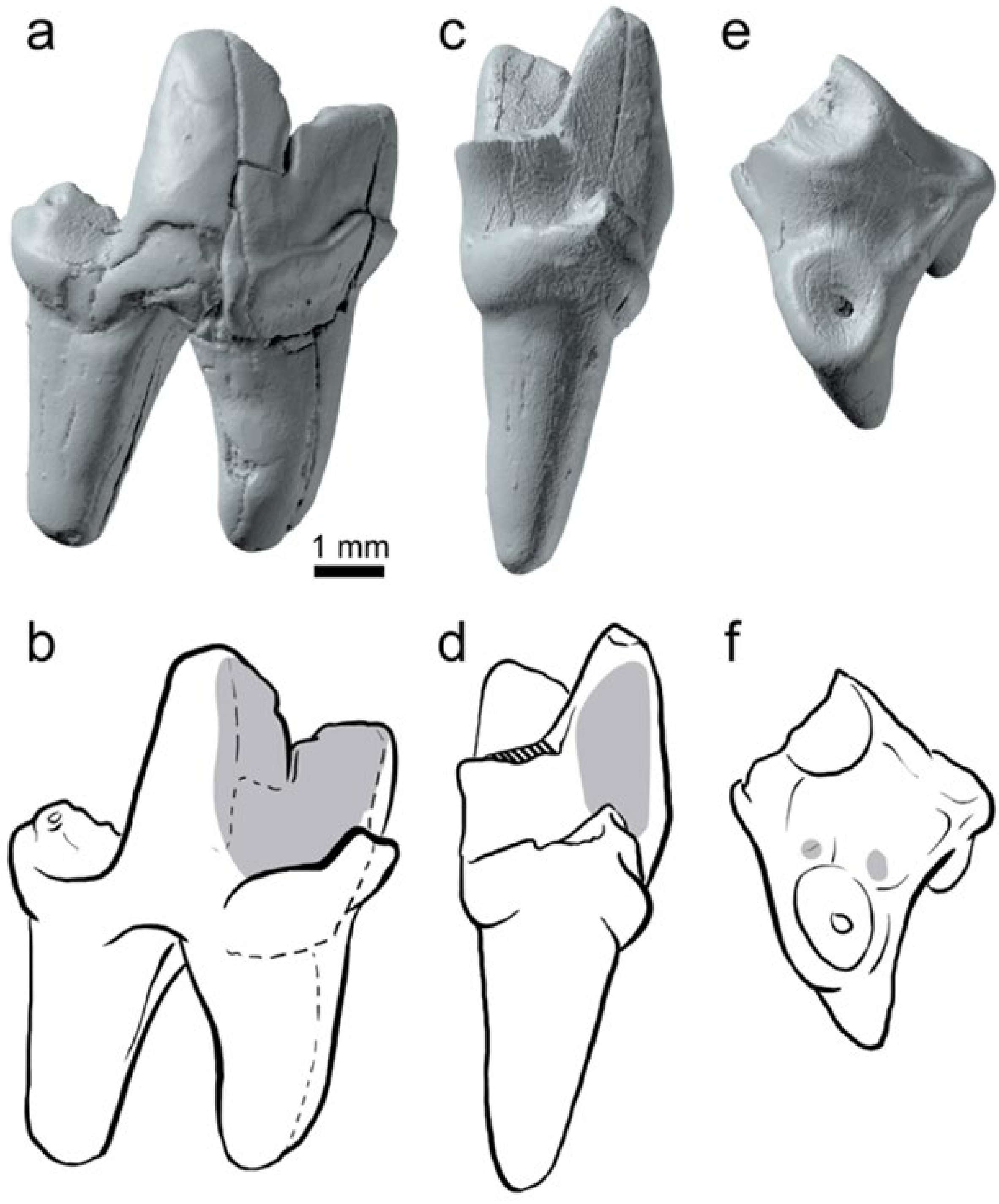

Figure 3. Wear facets on isolated teeth of *Africtis sirtensis*, gen. et sp. nov., from the early Oligocene of central Libya. (a-b) holotype right M_1 of *Africtis sirtensis* (Z7I-11) in buccal view, with shearing facet on mesiobuccal trigonid highlighted (b). (c-d) holotype right M_1 of *Africtis sirtensis* (Z7I-11) in distal view, with shearing facet on postvallid highlighted (d). (e-f) right P^4 of *Africtis sirtensis* (Z7I-171) in occlusal view, with wear facets for occlusion with posterior accessory cusps of P_4 highlighted (f).

Hyainailouroid Comparisons:

Hyainailouroidea is a superfamily that includes nearly all Afro-Arabian members of Hyaenodonta (Rana et al., 2015; Borths et al., 2016), as well as several genera that dispersed into parts of Laurasia during the Paleogene (Borths and Stevens, 2019). It is further divided into three subfamilies: Teratodontinae (sensu Borths et al., 2016), Apterodontinae, and Hyainailourinae.

Teratodontinae – Teratodontines are known for possession of the following features: a widely-basined talonid and salient entoconid on lower molars; lower molar talonids that are lingually closed; a well-developed ectocingulid on lower molars; a bulbous and mesially directed protocone on P^4; absence of a parastyle on P^4; and a paracone and metacone that are distinctly separated on molars (from Solé et al., 2014b). Hence, *Africtis sirtensis* shares at least some features with teratodontines. Most notably, these include a well-developed M_1 ectocingulid, an inflated P^4 protocone, absence of the P^4 parastyle, and (likely) unfused upper molar paracone and metacone, as inferred from the wear facets on the talonid of Z7I-11. Still, *Africtis sirtensis* differs considerably in the size and complexity of the lower molar talonid, in addition to the various characteristics that ally it more so with carnivoramorphans (see below).

A reasonably compelling case could be made that Z7I-11 represents the distal molar (M_2 or M_3) of a small teratodontine, given the reduction of the talonid that occurs in distal molars of hyaenodonts, and the increased emphasis on postvallum/prevallid shear that occurs distally in the jaw. The genus *Masrasector* (Simons and Gingerich, 1974) makes a particularly apt comparison, in that it most closely approximates the size and mesocarnivorous morphology of

Africtis sirtensis among the teratodontines. However, the possibility that Z7I-11 represents M_2 or M_3 of Masrasector or a closely related teratodontine is unlikely given the reduction of the metaconid that coincides with talonid reduction in hyaenodont distal molars. Thus, if Z7I-11 were the M_2 or M_3 of a hyaenodont, it would likely possess a much smaller metaconid, if this cusp were present at all. *Africtis sirtensis* further differs from *Masrasector* specifically in its broader M_1 trigonid (due in part to its larger metaconid), narrower and shorter talonid, larger hypoconid, lack of an entoconid, more buccal position of the hypoconulid, and lack of a metacone on dP^3.

Hyainailouridae – Hyainailouridae is an amalgamation of the subfamilies Apterodontinae and Hyainailourinae (Borths et al., 2016). Apterodontinae is a relatively non-diverse subfamily containing only the genera *Apterodon* and *Quasiapterodon* (Grohé et al., 2012). Hyainailourines, by contrast, are the largest hyaenodont subfamily in terms of their generic diversity (Solé et al., 2015; Borths and Stevens, 2019). Both clades are united by the extreme reduction, and in many cases complete loss, of the lower molar metaconids, as well as their reduction and simplification of the lower molar talonid. While the latter of these features is shared with *Africtis sirtensis*, the vestigial nature of the hyainailourid metaconid contrasts markedly from the condition in *Africtis sirtensis*. Even primitive hyainailourid taxa, such as *Kerberos langebadreae* (Solé et al., 2015) and *Orienspterodon dahkoensis* (Chow, 1975; Egi et al., 2007), possess more secant lower molars, which Solé et al. (2014b) cite as a hallmark of Hyaenodonta, as opposed to Carnivora. Even so, various P^4 features are shared between *A. sirtensis* and the hyainailourids *Metapterodon* and *Isohyaenodon*, including the reduction of the parastyle, and the slight mesial displacement of the protocone. The lower dentition of these taxa, however, bear few resemblances, as both *Metapterodon* and *Isohyaenodon* are characterized by hypercarnivorous lower molars, including the complete absence of the M_1 metaconid, fully trenchant carnassial crests, and the vestigial talonid. These features contrast starkly with the M_1 of *Africtis sirtensis*.

Hyainailouroid dP3 – Currently, too few hyainailouroid dP3 specimens have been described to document diagnostic features among its subgroups, but preliminary comparisons with Z7I-172 are possible at this stage. This is due in large part to the work of Borths and Stevens (2017b), who described and compared the deciduous premolars of various hyainailouroid genera, revealing considerable variation within the group. Other works describing deciduous premolars of hyainailouroids include: Morales et al. (2010), Solé et al. (2016b), Borths and Seiffert (2017), and Borths and Stevens, 2017, Borths and Stevens, 2017. To date, eight genera of hyainailouroids preserve dP^3: *Metasinopa* Osborn 1909, *Masrasector* Simons and Gingerich 1974, *Dissopsalis* Pilgrim 1910, *Anasinopa* Savage 1965, *Leakitherium* Savage 1965, *Pakakali* Borths and Stevens, 2017, *Prionogale* Schmidt-Kittler and Heizmann 1991, and possibly *Namasector* Morales et al., 2008 (reinterpreted by Borths and Stevens, 2017). *Africtis sirtensis* differs from all published hyainailouroid dP^3's in several notable ways: the absence of the metacone, the extreme reduction of the protocone and talon basin, and the enlargement of the metastyle. It further differs from hyainailouroid dP^3's by its reduction or absence of the parastyle, but this is likely an autapomorphous feature, as all other documented carnivoramorphan dP^3's still retain a parastyle. The closest resemblance to the dP^3 morphology found in *Africtis sirtensis* among hyainailouroids is that of *Metasinopa*, which possesses dP^3 with an elongate metastyle and a reduced protocone. Even so, the morphology of dP^3 in *Metasinopa* does not approach the extreme conditions found in *Africtis sirtensis*. The dP^3 of *Metasinopa* further differs from that of *Africtis sirtensis* by its retention of a metacone.

Carnivoramorphan comparisons:

Surprisingly, the carnassial morphology of *Africtis sirtensis* suggests a closer affiliation with carnivoramorphans (viverravids + carnivoraforms) than the hyainailouroideans that dominated African faunas throughout the Paleogene (Lewis and Morlo, 2010). This assessment is based on multiple characters and character-inferences that collectively point toward the same conclusion. Chiefly, they are: the presence (retention) of a large metaconid on M_1; the mesiobuccal shearing facet on the M_1 trigonid; the mesiodistal, rather than dorsoventral, orientation of the precingulid on M_1; the reduced length of the M_1 talonid; the large, robust, and mesially shifted M_1 hypoconid; the buccal placement of the M_1 hypoconulid (as inferred from the small hypoconulid lobe); the buccal expansion/transverse orientation of the P^4 metastyle; the presence of two shearing facets between the paracone and protocone of P^4; the lack of a metacone on P^4 and dP^3; the reduced or absent trigon basin on P^4 and dP^3; the greatly reduced (virtually absent) protocone on dP^3; the hypertrophy of the dP^3 metastyle; and the absence of a buccal cingulum on dP^3. All of these characters distinguish *Africtis sirtensis* from the contemporaneous hyainailouroideans present in Afro-Arabia.

Establishing precisely where *Africtis sirtensis* fits within Carnivoramorpha is a more difficult question. This is especially the case given the paucity of available material for *Africtis* *sirtensis*, the complete lack of carnivoramorphans definitively known from the Paleogene of Africa, and the relative dearth of basal carnivoramorphan dP^3's in the fossil record (effectively restricting intraordinal comparisons to two tooth loci, rather than three). As such, no attempt to conduct a formal phylogenetic analysis will be made here. Nonetheless, we provisionally identify *Africtis sirtensis* as a basal carnivoraform based on the broad comparisons detailed below.

Crown Carnivora – Crown carnivorans first appear in the fossil record in the middle Eocene of Laurasia (Wesley-Hunt and Flynn, 2005), but these animals do not demonstrably arrive in Africa until the early Miocene (Rasmussen and Gutierrez, 2009; Werdelin and Peigné, 2010). Both major subclades of crown carnivorans, the feliforms and caniforms, invade Africa at this time. Feliforms, ostensibly the more diverse of the two groups in Africa (Werdelin and Peigné, 2010), are known for possessing large protocones on P^4, as well as considerable enlargement of the P^4 parastyle (Flynn and Galiano, 1982). While *Africtis sirtensis* unquestionably retains a large P^4 protocone, the marked suppression or near absence of the parastyle suggests a more basal position within Carnivoraformes, although Wesley-Hunt and Flynn (2005) reported some early diverging feliforms with reduced P^4 parastyles. Among the feliforms, numerous taxa are present in Africa by at least the early Miocene, including predominantly viverroid carnivorans such as viverrids, herpestids, and stenoplesictids. *Mioprionodon hodopeus*, once thought to be the earliest carnivoramorphan to reach Africa (Rasmussen and Gutierrez, 2009), differs from *Africtis sirtensis* in its more secant M_1 morphology, including its hypertrophied trigonid crests, its smaller metaconid base, and its smaller hypoconid. Other viverroids, such as the stenoplesictids

Africanictis and *Moghradictis*, differ from *Africtis sirtensis* in much the same way: the more secant morphology of their carnassial teeth precludes them from any close affinity. The earliest herpestids, by contrast, consistently differ from *Africtis sirtensis* in their elongated and elaborate M_1 talonid morphologies (the expanded basins, and the hypertrophied talonid cusps, including the entoconid). This is true for genera such as *Herpestes*, *Leptoplesictis*, *Ugandictis*, *Kichechia*, and *Legetetia*, all known from the early or middle Miocene of eastern Africa (Werdelin and Peigné, 2010). Caniform carnivorans, including the early and middle Miocene African amphicyonids, reduce their P^4 parastyle and protocone, and are diagnostic in the extreme mesial displacement of the P^4 protocone (Flynn and Galiano, 1982; Wesley and Flynn, 2003). While *Africtis sirtensis* shares with caniforms the reduction of the parastyle, it differs in both the size and location of the P^4 protocone. Importantly, in all cases where *Africtis sirtensis* differs from crown carnivorans, it bears the primitive character state: a large, centrally placed P^4 protocone, and a reduced P^4 parastyle. This pattern suggests a more basal placement among the Carnivoramorpha.

Viverravidae – Viverravids are generally regarded as the most basal members of Carnivoramorpha (Wesley-Hunt and Flynn, 2005; Wesley-Hunt and Werdelin, 2005; Polly et al., 2006). Their carnassial morphology often reflects this basal placement, with P^4 possessing perhaps the most distinctive characteristics relative to other carnivoramorphans. Specifically, the P^4 of viverravids is known for: a well-developed parastyle lacking basal cingula; a nearly vertical paracone that is poorly excavated on its mesiolingual surface; a weakly trenchant preparacrista that is not deflected lingually; a weakly trenchant, buccally oriented metastyle with a narrow carnassial notch; a distally situated protocone that is only slightly mesial to the apex of the paracone; poorly-developed protocone cristae; a prominent mesial embayment between the paracone and the large parastyle; and poorly developed basal cingula (Fox and Youzwyshyn, 1994). Importantly, these are all considered primitive features among carnivoramorphans (Fox and Youzwyshyn, 1994). In the lower dentition, diagnostic features of viverravids that are relevant to this discussion are restricted to P_4, given that many carnivoramorphans share a similar M_1 morphology (distinctions can be made based purely on the number of molars, however). The P_4 of viverravids is diagnostic among carnivoramorphans in the presence of one, rather than two posterior accessory cusps, with the exception of *Didymictis* and *Protictis* (Flynn and Galiano, 1982; Gheerbrant, 1995). The deciduous dental morphology of viverravids, and particularly that of dP^3, is almost entirely unknown, with the lone exception being the work of Zack (2012), who described the deciduous premolar morphology of *Didymictis protenus*. As such, the data are not sufficient for comparison. With regards to P^4 and P_4, *Africtis sirtensis* shares several similarities with viverravids, including: poorly developed P^4 basal cingula and protocone cristae; the near-vertical orientation of the P^4 paracone; the weakly trenchant P^4 metastyle and preparacrista; and the distal location of the P^4 paracone. It differs from viverravids, however, in the weak development of the P^4 parastyle and the (inferred) presence of two posterior accessory cusps on P_4. Both features indicate a more derived state for *Africtis sirtensis* and seem to ally it with basal carnivoraforms instead (the reduced P^4 parastyle is a derived state among viverravids, but a primitive state among carnivoraforms; Flynn and Galiano, 1982; Gheerbrant, 1995).

Basal Carnivoraformes – Establishing generalities among basal carnivoraforms has proven difficult, given that the group is defined largely on the absence of synapomorphies present in other carnivoramorphan clades (Flynn and Galianio, 1982; Wesley-Hunt and Flynn, 2005). *Africtis sirtensis* is no exception. It shares with basal carnivoraforms the reduction of the P^4 parastyle (Wortman and Matthew, 1899; Matthew, 1909; Flynn and Galiano, 1982), a more distal position of the P^4 protocone (Wesley and Flynn, 2003), and it is inferred to have had two posterior accessory cusps on P_4 (Flynn and Galiano, 1982; Gheerbrant, 1995), while lacking many of the carnassial features diagnostic of crown carnivorans. *Africtis sirtensis* does not show convincing morphological affinities with any established Eurasian basal carnivoraform taxa, and can be distinguished quite readily from them. It differs from *Gracilocyon* (Smith and Smith, 2010) based on its lower, more robust, and less trenchant m1 trigonid cusps, although the talonid morphology appears superficially similar (narrow buccolingual width, absence of the entoconid, large, mesially located hypoconid). *Africtis sirtensis* shares with *Dormaalocyon* (Solé et al., 2014a) the absence of a P^4 parastyle, but differs in its weaker development of the P^4 preparacrista, more bunodont P^4 protocone, and more reduced M_1 talonid, both in terms of size and number of cusps. It differs from *Vassacyon* (Matthew, 1909) similarly in its reduction of the M_1 talonid, including a narrower and shallower talonid without a distinct entoconid; it further differs from *Vassacyon* by its greater inflation of the P^4 paracone and protocone. *Africtis sirtensis* differs from *Uintacyon* (Leidy, 1872) by the larger size of its M_1 hypoconid, the absence of the M_1 entoconid, and the shorter, more robust nature of its M_1 trigonid cusps.

The genus *Miacis* has long been considered a wastebasket taxon (Wang and Tedford, 1994), complicating the erection of morphological synapomorphies for the group. The most logical comparisons come from Eurasian members of the genus, which include *M. lushiensis* (Chow, 1975), *M. thailandicus* (Ducrocq et al., 1992), *M. boqinghensis* (Huang et al., 1999), and *M. invictus* (Matthew and Granger, 1925). Heinrich et al. (2008) asserted that *M. lushiensis* and *M. thailandicus* are more likely related to the Asian genus *Xinyuictis* (Zheng et al., 1975), rather than other members of *Miacis*. Nonetheless, the carnassials of these particular taxa do not obviously bear much resemblance to *Africtis sirtensis*, as they all generally possess a larger and more prominent M_1 talonid, with smaller hypoconids and larger entoconids. *Xinyuictis*, from the early Eocene of China, differs from *Africtis sirtensis* in its hypercarnivorous morphology of P^4, including a tall, pointed paracone with well-developed pre- and postparacristae (Zheng et al., 1975). *Zodiocyon* (Tong and Wang, 2006), another basal carnivoraform from the early Eocene of China, is similar in size to *Africtis sirtensis* on the basis of its M_1. It differs, however, in the small size of its hypoconid, which is virtually indistinguishable from the cristid obliqua.

Discussion:

The presence of a carnivoraform in Africa during the early Oligocene is surprising for a number of reasons. First and foremost, *Africtis sirtensis* documents the earliest occurrence of the carnivoramorphan clade in Africa, antedating its prior definitive first appearance at the earliest Miocene site of Nakwai in northwestern Kenya by ~8–9 Ma (Rasmussen and Gutierrez, 2009; Coster et al., 2015a). Second, the new Libyan taxon may well be the only known occurrence of a basal carnivoraform on the African continent. These animals were otherwise restricted to Laurasia, where they were diverse, widespread, and fairly ubiquitous during the late Paleocene and Eocene. If our provisional identification of *Africtis* as a basal carnivoraform is corroborated by further anatomical data, the temporal range of basal carnivoraforms would be extended into the early Oligocene, indicating that at least one basal carnivoraform survived the climatic and paleoenvironmental changes coinciding with the Eocene-Oligocene boundary.

Biogeographically, the early Oligocene occurrence of *Africtis sirtensis* implies that the earliest African carnivoraforms must have colonized Africa by rafting rather than dispersal across a land bridge, because the tectonic collision between Africa and Eurasia did not occur until sometime near the Oligocene-Miocene boundary (Kappelman et al., 2003; McQuarrie and van Hinsbergen, 2013). Indeed, given that basal carnivoraforms are unknown from the Oligocene of Laurasia, it seems most likely that the ancestors of *Africtis sirtensis* dispersed to Africa during the latter part of the Eocene rather than during the earliest Oligocene. The warmer and wetter climatic conditions of the Eocene would have been far more conducive for sweepstakes dispersal of a small carnivoraform across a Tethyan marine barrier than the cooler and drier climate prevailing in the Oligocene (Beard, 2016). It is notable that hyainailouroids successfully crossed this barrier during the Eocene as well (Gheerbrant and Rage, 2006), indicating a greater degree of faunal connectivity between Africa and Eurasia at that time than would be expected otherwise. Whatever the exact timing of their dispersal, *Africtis sirtensis* and the crown carnivoran ancestors of euplerids and herpestids indicate that the early colonization of Africa by Eurasian carnivoraforms was not monophyletic, but instead occurred in multiple iterations. This pattern resembles the repeated invasions of Africa, Madagascar and South America by primates traversing marine barriers (Beard, 2016; Gunnell et al., 2018; Seiffert et al., 2020). Finally, the unexpected occurrence of a basal carnivoraform in the Zallah Incision local fauna adds a highly distinctive element to this central Libyan fauna, underscoring the biogeographic provincialism that characterized early Oligocene mammal faunas across northern Afro-Arabia (Coster et al., 2015a, Coster et al., 2015b; Beard et al., 2016, 2017).

An important caveat concerning many of the points raised here is the paucity of anatomical information that is currently available for *Africtis sirtensis*, and, to a certain extent, other elements of the Zallah Incision local fauna. This fauna was collected during reconnaissance exploration of Paleogene outcrops in the vicinity of Zallah Oasis in early 2013, during an interval of significant regional political upheaval and insecurity. Under more normal conditions, it would almost certainly be possible to sample this promising fauna more thoroughly and obtain more nearly complete specimens of *Africtis sirtensis* and co-occurring taxa. We look forward to the time when further work on the Zallah Incision local fauna becomes feasible, enabling more detailed understanding of the anatomy, phylogenetic relationships, and evolutionary history of Africa's oldest known carnivoramorphan.

References

Beard KC. 2016. Out of Asia: anthropoid origins and the colonization of Africa. Annu. Rev. Anthropol. 45: 199-213.

Beard KC, Coster PMC, Salem MJ, Chaimanee Y, Jaeger J-J. 2016. A new species of Apidium (Anthropoidea, Parapithecidae) from the Sirt Basin, central Libya: first record of Oligocene primates from Libya. J. Hum. Evol. 90: 29-37.

Beard KC, Coster PMC, Salem MJ, Chaimanee Y, Jaeger J-J. 2017.Biogeographic provincialism shown by Afro-Arabian mammals during the middle Cenozoic: climate change, Red Sea rifting, and global eustasy. In: Agius, D.A., Khalil, E., Scerri, E.M.L., Williams, A. (Eds.), Human Interaction with the Environment in the Red Sea. Brill, Leiden, The Netherlands, pp. 48-68.

Borths MR, Seiffert ER. 2017. Craniodental and humeral morphology of a new species of Masrasector (Teratodontinae, Hyaenodonta, Placentalia) from the late Eocene of Egypt and locomotor diversity in hyaenodonts. PLoS One 12: e0173527.

Borths MR, Stevens NJ. 2017a. The first hyaenodont from the late Oligocene Nsungwe Formation of Tanzania: paleoecological insights into the PaleogeneNeogene carnivore transition. PLoS One 12: e0185301.

Borths MR, Stevens NJ. 2017b. Deciduous dentition and dental eruption of Hyainailouroidea (Hyaenodonta, “Creodonta,” Placentalia, Mammalia). Palaeontol. Electron. 20: 55A.

Borths MR, Stevens NJ. 2017c. Taxonomic affinities of the enigmatic Prionogale breviceps, early Miocene, Kenya. Hist. Biol. 31: 784-793.

Borths MR, Stevens NJ. 2019. Simbakubwa kutokaafrika, gen. et sp. nov. (Hyainailourinae, Hyaenodonta, 'Creodonta,' Mammalia), a gigantic carnivore from the earliest Miocene of Kenya. J. Vertebr. Paleontol. 39: e1570222.

Borths MR, Holroyd PA, Seiffert ER. 2016. Hyainailourine and teratodontine cranial material from the late Eocene of Egypt and the application of parsimony and Bayesian methods to the phylogeny and biogeography of Hyaenodonta (Placentalia, Mammalia). PeerJ 4: e2639.

Butler PM. 1946. The evolution of carnassial dentitions in the Mammalia. Proc. Zool. Soc. Lond. 116: 198-220.

Butler PM. 1952. The milk-molars of Perissodactyla, with remarks on molar occlusion. Proc. Zool. Soc. Lond. 121: 777-817.

Chow M. 1975. Some carnivores from the Eocene of China. Vertebr. Palasiat. 13: 165-168.

Coster PMC, Beard KC, Salem MJ, Chaimanee Y, Brunet M, Jaeger J-J. 2015a. A new early Oligocene mammal fauna from the Sirt Basin, central Libya: biostratigraphic and paleobiogeographic implications. J. Afr. Earth Sci. 104: 43-55.

Coster PMC, Beard KC, Salem MJ, Chaimanee Y, Jaeger J-J. 2015b. New fossils from the Paleogene of central Libya illuminate the evolutionary history of endemic African anomaluroid rodents. Front. Earth Sci. 3: 56.

Crochet J-Y, Peigné S, Mahboubi M. 2001. Ancienneté des Carnivora (Mammalia) en Afrique. In: Denys, C., Granjon, L., Poulet, A. (Eds.), African Small Mammals. IRD Editions, Paris, pp. 91-100.

Ducrocq S, Buffetaut E, Buffetaut-Tong H, Helmckke-Ingavat R, Jaeger, J-J, Jongkanjanasoontorn Y, Suteethorn V. 1992. A lower Tertiary vertebrate fauna from Krabi (South Thailand). Neues Jahrbuch Geol. Palaontol. Abhand. 184: 101-122.

Egi N, Tsubamoto T, Takai M. 2007. Systematic status of Asian “Pterodon” and early evolution of hyaenaelurine hyaenodontid creodonts. J. Paleontol. 81: 770-778.

Eizirik E, Murphy WJ, Koepfli K-P, Johnson WE, Dragoo JW, Wayne RK, O’Brien SJ. 2010. Pattern and timing of diversification of the mammalian order Carnivora inferred from multiple nuclear gene sequences. Mol. Phylogenet. Evol. 56: 49-63.

Flynn JJ, Galiano H. 1982. Phylogeny of early Tertiary Carnivora, with a description of a new species of Protictis from the middle Eocene of northwestern Wyoming. Am. Mus. Novit. 2725: 1-64.

Flynn JJ, Finarelli JA, Spaulding M. 2010. Phylogeny of the Carnivora and Carnivoramorpha, and the use of the fossil record to enhance understanding of evolutionary transformations. In: Goswami, A., Friscia, A. (Eds.), Carnivoran Evolution: New Views on Phylogeny, Form, and Function. Cambridge University Press, Cambridge, pp. 25-63.

Fox RC, Youzwyshyn GP. 1994. New primitive carnivorans (Mammalia) from the Paleocene of western Canada, and their bearing on relationships of the order. J. Vertebr. Paleontol. 14: 382-404.

Fox RC, Scott CS, Rankin BD. 2010. New early carnivoran specimens from the Puercan (earliest Paleocene) of Saskatchewan, Canada. J. Paleontol. 84: 1035-1039.

Gheerbrant E. 1995. Les mammiféres Paléocénes du Bassin d'Ourzazate (Maroc). III. Adapisoriculidae et autres mammiféres (Carnivora, ?Creodonta, Condylarthra, ?Ungulata et incertae sedis). Palaeontograph. Abteilung A 237: 39-132.

Gheerbrant E, Rage JC. 2006. Paleobiogeography of Africa: how distinct from Gondwana and Laurasia? Palaeogeogr. Palaeoclimatol. Palaeoecol. 241: 224-246.

Grohé C, Morlo M, Chaimanee Y, Blondel C, Coster P, Valentin X, Salem M, Bilal AA, Jaeger J-J, Brunet M. 2012. New Apterodontinae (Hyaenodontida) from the Eocene locality of Dur At-Talah (Libya): systematic, paleoecological and phylogenetical implications. PLoS One 7: e49054.

Gunnell GF, Boyer DM, Friscia AR, Heritage S, Manthi FK, Miller ER, Sallam HM, Simmons NB, Stevens NJ, Seiffert ER. 2018. Fossil lemurs from Egypt and Kenya suggest an African origin for Madagascar's aye-aye. Nat. Commun. 9: 1-12.

Heinrich RE, Strait SG, Houde P. 2008. Earliest Eocene Miacidae (Mammalia: Carnivora) from northwestern Wyoming. J. Paleontol. 82: 154-162.

Huang X-S, Tong Y-S, Wang J-W. 1999. A new Miacis (Mammalia, Carnivora, Miacidae) from the middle Eocene of Yuanqu Basin, Shanxi Province. Vertebr. Palasiat. 37: 291-299.

Kappelman J, Rasmussen DT, Sanders WJ, Feseha M, Bown T, Copeland P, Crabaugh J, Fleagle J, Glantz M, Gordon A, Jacobs B, Maga M, Muldoon K, Pan A, Pyne L, Richmond B, Ryan T, Seiffert ER, Sen S, Todd L, Wiemann MC, Winkler A. 2003. Oligocene mammals from Ethiopia and faunal exchange between Afro-Arabia and Eurasia. Nature 426: 549-552.

Leidy J. 1872. Remarks on fossils from Wyoming. Proc. Acad. Nat. Sci. Philadelphia 24: 277.

Lewis ME, Morlo M. 2010. Creodonta. In: Werdelin, L., Sanders, W.J. (Eds.), Cenozoic Mammals of Africa. University of California Press, Berkeley, pp. 543-560.

Matthew WD, 1909. The Carnivora and Insectivora of the Bridger Basin, middle Eocene. Mem. Am. Mus. Nat. Hist. 9: 291-567.

Matthew WD, Granger W. 1925. New mammals from the Irdin Manha Eocene of Mongolia. Am. Mus. Novit. 198: 1-10.

McQuarrie N, van Hinsbergen DJJ. 2013. Retrodeforming the Arabia-Eurasia collision zone: age of collision versus magnitude of continental subduction. Geology 41: 315-318.

Mellett JS, 1977. Paleobiology of North American Hyaenodon (Mammalia, Creodonta). Contrib. Vertebr. Evol. 1: 1-134.

Morales J, Pickford M, Salesa MJ. 2008. Creodonta and Carnivora from the early Miocene of the northern Sperrgebiet, Namibia. Mem. Geol. Surv. Namibia 20: 291-310.

Morales J, Brewer P, Pickford M. 2010. Carnivores (Creodonta and Carnivora) from the basal middle Miocene of Gebel Zelten, Libya, with a note on a large amphicyonid from the middle Miocene of Ngorora, Kenya. Bull. Tethys Geol. Soc., Cairo 5: 43-54.

Osborn HF. 1909. New carnivorous mammals from the Fayum Oligocene, Egypt. Bull. Am. Mus. Nat. Hist. 26: 415-424.

Pilgrim GE. 1910. Notices of new mammalian genera and species from the Tertiaries of India. Rec. Geol. Surv. India 40: 63-71.

Polly PD, Wesley-Hunt GD, Heinrich RE, Davis G, Houde P. 2006. Earliest known carnivoran auditory bulla and support for a recent origin of crown-group Carnivora (Eutheria, Mammalia). Palaeontology 49: 1019-1027.

Rana RS, Kumar K, Zack SP, Solé F, Rose KD, Missiaen P, Singh L, Sahni A, Smith T. 2015. Craniodental and postcranial morphology of Indohyaenodon raoi from the early Eocene of India, and its implications for ecology, phylogeny, and biogeography of hyaenodontid mammals. J. Vertebr. Paleontol. 35: e965308.

Rasmussen DT, Gutierrez M. 2009. A mammalian fauna from the late Oligocene of northwestern Kenya. Palaeontograph. Abteilung A 288: 1-52.

Rasmussen DT, Friscia AR, Gutierrez M, Kappelman J, Miller ER, Muteti S, Reynoso D, Rossie JB, Spell TL, Tabor NJ, Gierlowski-Kordesch E, Jacobs BF, Kyongo B, Macharwas M, Muchemi F. 2019. Primitive Old World monkey from the earliest Miocene of Kenya and the evolution of cercopithecoid bilophodonty. Proc. Natl. Acad. Sci. USA 116: 6051-6056.

Rolland J, Condamine FL, Beeravolu CR, Jiguet F, Morlon H. 2015. Dispersal is a major driver of the latitudinal diversity gradient of Carnivora. Global Ecol. Biogeogr. 24: 1059-1071.

Savage RJG. 1965. Fossil mammals of Africa 19: The Miocene Carnivora of East Africa. Bull. Br. Mus. Nat. Hist. (Geol.) 10: 239-316.

Schmidt-Kittler N, Heizmann PJ. 1991. Prionogale breviceps n. gen. n. sp.: evidence of an unknown major clade of eutherians in the lower Miocene of East Africa. Münchner Geowiss. Abh. A Geol. Palaontol. 19: 5-16.

Seiffert ER. 2006. Revised age estimates for the later Paleogene mammal faunas of Egypt and Oman. Proc. Natl. Acad. Sci. USA 103: 5000-5005.

Seiffert ER, Tejedor MF, Fleagle JG, Novo NM, Cornejo FM, Bond M, de Vries D, Campbell Jr. KE. 2020. A parapithecid stem anthropoid of African origin in the Paleogene of South America. Science 368: 194-197.

Simons EL, Gingerich PD. 1974. New carnivorous mammals from the Oligocene of Egypt. Ann. Geol. Surv. Egypt 4: 157-166.

Smith T, Smith R. 2010. A new 'miacid' carnivoran from the earliest Eocene of Europe and North America. Acta Palaeontol. Pol. 55: 761-764.

Solé F. 2014. New carnivoraforms from the early Eocene of Europe and their bearing on the evolution of the Carnivoraformes. Palaeontology 57: 963-978.

Solé F, Essid EM, Marzougui W, Temani R, Ammar HK, Mahboubi M, Marivaux L, Vianey-Liaud M, Tabuce R. 2016b. New fossils of Hyaenodonta (Mammalia) from the Eocene localities of Chambi (Tunisia) and Bir el Ater (Algeria), and the evolution of the earliest African hyaenodonts. Palaeontol. Electron. 19: 41A.

Solé F, Gheerbrant E, Amaghzaz M, Bouya B. 2009. Further evidence of the African antiquity of hyaenodontid ('Creodonta', Mammalia) evolution. Zool. J. Linn. Soc. 156: 827-846.

Solé F, Amson E, Borths MR, Vidalenc D, Morlo M, Bastl K. 2015. A new large hyainailourine from the Bartonian of Europe and its bearings on the evolution and ecology of massive hyaenodonts (Mammalia). PLoS One 10: e141941.

Solé F, Lhuillier J, Adaci M, Bensalah M, Mahboubi M, Tabuce R. 2014b. The hyaenodontidans from the Gour Lazib area (?early Eocene, Algeria): implications concerning the systematics and the origin of the Hyainailourinae and Teratodontinae. J. Syst. Palaeontol. 12: 303-322.

Solé F, Smith R, Coillot T, De Bast E, Smith T. 2014a. Dental and tarsal anatomy of 'Miacis' latouri and a phylogenetic analysis of the earliest carnivoraforms (Mammalia, Carnivoramorpha). J. Vertebr. Paleontol. 31: 1-21.

Solé F, Smith T, De Bast E, Codrea V, Gheerbrant E. 2016a. New carnivoraforms from the latest Paleocene of Europe and their bearing on the origin and radiation of Carnivoraformes (Carnivoramorpha, Mammalia). J. Vertebr. Paleontol. 36: e1082480.

Spaulding M, Flynn JJ. 2012. Phylogeny of the Carnivoramorpha: the impact of postcranial characters. J. Syst. Palaeontol. 10: 653-677.

Spaulding M, Flynn JJ, Stucky RK. 2010. A new basal carnivoramorphan (Mammalia) from the 'Bridger B' (Black's Fork member, Bridger Formation, Bridgerian NALMA, middle Eocene) of Wyoming, USA. Palaeontology 53: 815-832.

Tong Y-S, Wang J-W. 2006. Fossil mammals from the early Eocene Wutu Formation of Shandong Province. Palaeontol. Sinica (New Series C) 28: 1-195.

Wang X-M, Tedford RH. 1994. Basicranial anatomy and phylogeny of primitive canids and closely related miacids (Carnivora: Mammalia). Am. Mus. Novit. 3092: 1-34.

Werdelin L, Peigné S. 2010. Carnivora. In: Werdelin, L., Sanders, W.J. (Eds.), Cenozoic Mammals of Africa. University of California Press, Berkeley, pp. 603-657.

Wesley GD, Flynn JJ. 2003. A revision of Tapocyon (Carnivoramorpha), including analysis of the first cranial specimens and identification of a new species. J. Paleontol. 77: 769-783.

Wesley-Hunt GD, Flynn JJ. 2005. Phylogeny of the Carnivora: basal relationships among the carnivoramorphans, and assessment of the position of 'Miacoidea' relative to Carnivora. J. Syst. Palaeontol. 3: 1-28.

Wesley-Hunt GD, Werdelin L. 2005. Basicranial morphology and phylogenetic position of the upper Eocene carnivoramorphan Quercygale. Acta Palaeontol. Pol. 50: 837-846.

Wortman JL, Matthew WD. 1899. The ancestry of certain members of the Canidae, Viverridae, and Procyonidae. Bull. Am. Mus. Nat. Hist. 12: 109-138.

Wyss AR, Flynn JJ. 1993. A phylogenetic analysis and definition of the Carnivora. In: Szalay, F.S., Novacek, M.J., McKenna, M.C. (Eds.), Mammal Phylogeny, vol. 2. Springer-Verlag, New York, pp. 32-52.

Yoder AD, Burns MM, Zehr S, Delefosse T, Veron G, Goodman SM, Flynn JJ. 2003. Single origin of Malagasy Carnivora from an African ancestor. Nature 421: 734-737.

Zack SP. 2012. Deciduous dentition of Didymictis (Carnivoramorpha: Viverravidae): implications for the first appearance of “Creodonta”. J. Mammal. 93: 808-817.

Zheng J, Tung Y, Qi H. 1975. Discovery of Miacidae (Carnivora) in Yuanshui Basin, Kiangsi Province. Vertebr. Palasiat. 13: 96-104.

Chapter 3

The Great Old World Biotic Interchange: a Quantitative Analysis of Mammalian Exchange at the Paleogene-Neogene Boundary

Spencer Mattingly and K. Christopher Beard

Abstract:

The Great Old World Biotic Interchange (GOWBI) was a biotic exchange event that occurred between Africa and Eurasia in the early Miocene, approximately 20 Ma. This exchange was catalyzed by the formation of a series of ephemeral landbridges that permitted, for the first time, the movement of land mammals back and forth. In doing so, it ended the long period of isolation and endemicity on the African mainland. Many parallels can hence be drawn to the younger, more famous episode of intercontinental exchange, the Great American Biotic Interchange (GABI). The present study applied quantitative measures of diversity, biogeography, and evolution to the GOWBI, using the GABI as a template. Using published occurrence data across four geologic stages in the Oligocene and early Miocene, we assessed the faunas of both landmasses through the context of their constituent ancestral origins. Total generic and family level diversities, numbers of dispersal events in both directions, numbers of subsequent originations and extirpations, and rates of origination and extirpation between endemic and immigrant lineages were tabulated. Results show that the GOWBI was in many ways similar to the GABI, including a dramatic upheaval of the endemic African fauna, but an almost negligible effect on the larger, more diverse Eurasian fauna. Asymmetry in the GOWBI was due primarily to the rapid dispersal and diversification of Eurasian genera in the early

Miocene of Africa, instead of disproportionately large extirpation rates among African natives. The results indicate a repeated pattern of asymmetry in large scale intercontinental exchange events involving “island continents”.

Introduction:

Biotic interchange is an inevitable consequence of life on a dynamic planet. Although the intensity, scale, and results of biotic invasions can vary widely (Stigall, 2019), a common trend seems to have emerged suggesting the frequent asymmetry of such exchanges (Vermeij, 1991). Indeed, the Cenozoic fossil record of mammals contains no shortage of evidence regarding asymmetry in large-scale exchange events (e.g., Stehlin, 1910; Marshall et al., 1982; Beard, 2002, Datta-Roy and Karanth, 2009; Graham, 2018). Perhaps the most famous and best studied among them is the Great American Biotic Interchange (GABI; Stehli and Webb, 1985). The GABI comprises a series of iterative dispersal episodes between North and South America following the closure of the Isthmus of Panama, roughly 3 Ma (Woodburne, 2010). Decades of research on the GABI have produced a nearly unparalleled record, both quantitative and qualitative, of continental-scale biotic interchange and its myriad causes and effects (e.g., Webb, 1991; Webb, 2006; Bacon et al., 2015; Domingo et al., 2020). The fruits of this research have yielded at least one overwhelming consensus: the outcomes of this exchange had a more significant, and disproportionately negative effect on the native South American mammal fauna when compared to its North American counterpart. The exact cause(s) of this asymmetry, however, remains a matter of debate.

A common component of hypotheses regarding asymmetry in the GABI is the "splendid isolation" of South America throughout much of the Cenozoic, leading to the development of a highly endemic mammal fauna (Simpson, 1980). Intriguingly, Africa suffered much the same fate following its rifting from South America (collectively "West Gondwana") during the middle Cretaceous (Granot and Dyment, 2015; Gheerbrant and Rage, 2006). Both of these landmasses would then begin their northward trajectories, acting as island continents throughout the Paleogene, until their collision with a Laurasian landmass in the Neogene. In Africa, the endemic radiation of placental mammals yielded the placental mammal clade Afrotheria (Murphy et al., 2001; Tabuce et al., 2007). Members of the Afrotheria include six extant orders, including Proboscidea (elephants and relatives), Hyracoidea (hyraxes), Sirenia (manatees and dugongs), Tubulidentata (aardvarks), Tenrecoidea (tenrecs and golden moles), and Macroscelidea (elephant shrews), along with the extinct order Embrithopoda, (and possibly the phylogenetically enigmatic Ptolemaiida). While afrotheres, in combination with hyaenodontan "creodonts", dominated African faunas throughout the Paleogene, their diversity in the Neogene waned as a result of periodic, often asymmetric exchange with Eurasia (Gheerbrant and Rage, 2006; Rage and Gheerbrant, 2020). The single largest episode of this Eurasian-African interchange occurred around the start of the Burdigalian, approximately 20 Ma, heralded by the formation of a terrestrial isthmus linking the two landmasses known as the "Gomphothere landbridge" (Rögl 1999; Sanders and Miller, 2002; Harzhauser et al., 2007; Sen, 2013). The exchange itself, which apparently proceeded quite rapidly (Cote et al. 2018), became known as the Great Old World Biotic Interchange (GOWBI; Gheerbrant, 2001), in reference to its New World analogue.

Despite the widespread recognition of the GOWBI and its role in dramatically reshaping the African mammal fauna (e.g., Coryndon and Savage, 1973; Pickford, 1981; Kappelman et al., 2003; Gheerbrant and Rage, 2006; Rage and Gheerbrant, 2020), comparatively little attention has been placed on it relative to the GABI, especially with respect to quantitative measures of interchange and its subsequent effects. This is likely due to numerous factors obfuscating comprehensive studies of the African record, including: (a) the presumed dearth of sampling on the African mainland, sometimes referred to as the "African Gap" (O'Connor et al., 2006; Gottfried et al., 2009); (b) geographic biases that restrict a majority of Cenozoic localities to the northern and eastern margins of the continent (Seiffert, 2010; Werdelin, 2010); (c) unresolved classifications of many late Paleogene and early Neogene taxa, especially at the family level; and (d) poor temporal resolution of numerous localities. Even so, continuous work over the last decade has greatly refined and enhanced our knowledge of the Paleogene-Neogene transition in Africa (e.g., Rasmussen and Gutierrez, 2009; Ducrocq et al., 2010; Borths and Stevens, 2017; Cote et al., 2018; Friscia et al., 2020), though not all problems within the African record have yet been resolved.

The quality of recent work permits a more empirical, quantitative approach to analyzing patterns and processes within the GOWBI. This contribution explores such possibilities by analyzing the GOWBI within the quantitative framework put forward by Marshall et al. (1982) in describing the GABI. Specifically, we tabulate dispersal, origination, and extinction data for land mammals in both Africa and Eurasia during the late Paleogene and early Neogene, and assess overall symmetry during the initial strongest pulse of exchange.

Methods:

Temporal setting and dataset - A time interval comprising four geologic stages - the Rupelian, Chattian, Aquitanian, and Burdigalian - was used for this analysis. These intervals were selected for a variety of reasons: (a) they represent enough time pre- and post-interchange to understand the effects on altering local faunal dynamics; (b) they correlate very nearly to established land mammals ages on each participant continent (Van Couvering and Delson, 2020); (c) they are consistent across continents, allowing direct comparisons within each interval; (d) they align closely with the length of time analyzed in the GABI (approximately 10-15 m.y. prior to interchange, and 3-4 post-interchange), allowing for reasonable comparisons between events. Genus and family level occurrence data during these time intervals were gathered from a combination of The Paleobiology Database downloads (paleobiodb.org), the Cenozoic Mammals of Africa text (Werdelin and Sanders, 2010), and primary literature searches. The most recent downloads from the Paleobiology Database were completed on April 30th, 2021, using the following parameters: taxonomic classification = "Mammalia"; time intervals = Rupelian-Burdigalian; location = (a) Africa plus Saudi Arabia, Oman, Yemen, United Arab Emirates, and Israel, (b) Asia plus Europe minus Saudi Arabia, Oman, Yemen, United Arab Emirates, and Israel. The two resulting datasets were then cleaned based on the following criteria: (1) taxa must be identified at least at the genus level; (2) taxa must be land mammals (i.e., excluding sirenians, cetaceans, and chiropterans); (3) age of the source fauna/site must be confidently within the temporal parameters of the analysis (Rupelian-Burdigalian); and (4) genus name must be valid. The resulting occurrence data were then counted to ascertain the number of unique genera, and their first and last appearances within Africa and Eurasia, respectively. Importantly, the presence of genera in some stages was inferred if it occurred in the preceding and succeeding intervals. Each individual genus was then assigned a place of geographic origin (either Africa or Eurasia) based on its higher-level taxonomic affinities (i.e., ancestral origins) and evolutionary history. African taxa included all members of the Afrotheria, plus hyainailouroid hyaenodontans. Eurasian taxa included all members of the Euarchontoglires, and all members of the Laurasiatheria excluding hyanailouroid hyaenodontans. Thus, members of exclusively African rodent and primate families, such as pedetids and parapithecids, were still considered Eurasian immigrants based on their presumed ancestral origins. Hyainailouroid hyaneodontans were not, however, due to their obscure higher-level relationships and origins, and their long history in Africa dating back to the early Paleogene (Lewis and Morlo, 2010).

First occurrence classification - First occurrences in the fossil record are products of either the dispersal of an immigrant taxon, or the *in situ* evolution of an ancestral lineage (“primary” and “secondary” immigrants, respectively). In order to quantify these separately, the geographic occurrence of all immigrant taxa was mapped onto their phylogenies, and the number of independent dispersal events was estimated using parsimony. The phylogenies used for each determination are listed in Table 2. In many cases, a presumed ancestral dispersal was counted as a discrete event, with each subsequent lineage attributed to *in situ* evolution. Because ancestral dispersals were counted, this led to a total number of events (dispersals plus originations) that was greater than the number of discrete immigrant genera. In instances where phylogenetic data were not available, *in-situ* evolution was used as the default assumption (i.e., dispersals were monophyletic unless compelling evidence suggested otherwise). In numerous cases here, dispersals could be inferred simply based on the age and geographic location of occurrence data. The total numbers of both dispersals and originations were tabulated for each landmass throughout the four time intervals.

Origination/extirpation rates and rarefaction - Classic methods for calculating "speciation" (origination) and "extinction" (extirpation) rates were used, following the work of Marshall et al. 1982. This permitted direct comparisons of rates to the GABI, though these methods have been shown to be biased over long periods of geologic time (Foote, 1994). Thus, rates were calculated as proportional origination/extinction per m.y. (genera per genus per m.y.). A secondary consideration for the use of such simplistic formulae is the relative paucity of occurrence data from the Chattian and Aquitanian stages, particularly in Africa. The lack of data in these intervening stages makes more thorough methods, which largely rely on continuity among intervals, knowingly biased or misleading. To assess sampling biases across continents and time intervals, a rarefaction analysis using only observed occurrence data was conducted using the 'individual rarefaction' function in Paleontological Statistics software (PAST v. 4.07b; Hammer et al., 2001). Curves were computed based on the distribution of genera per family in each time interval, and on each landmass.

Results:

Diversity Data - The specified time window, which spanned across four geologic stages in the late Paleogene and early Neogene, comprised a total of 17.9 million years. Of these, approximately four million years were measured after the onset of the GOWBI in the Burdigalian. In total, data downloads from the Paleobiology database yielded 807 occurrences under the specified parameters in Africa, and a combined 7220 occurrences in Europe and Asia. After data cleaning, 233 unique genera were recorded for Africa across all time intervals, and 523 for Eurasia.

Table 1. Faunal dynamics of Africa and Eurasia during the late Paleogene and early Neogene. Parentheses within the table denote the number of families represented by genera in a given stage. Abbreviations are: Rup. = Rupelian; Cha. = Chattian; Aqu. = Aquitanian; Bur. = Burdigalian. The asterisk denotes a well-known instance of late Oligocene proboscidean dispersal to Eurasia which was not formally counted here due to insufficient taxonomic resolution.

	Africa				Eurasia			
	Rup.	**Cha.**	**Aqu.**	**Bur.**	**Rup.**	**Cha.**	**Aqu.**	**Bur.**
Duration (m.y.)	6.1	4.8	2.6	4.4	6.1	4.8	2.6	4.4
Number of genera								
African	30 (11)	16 (6)	20 (11)	39 (13)	3 (2)	1 (1)	1 (1)	10 (5)
Eurasian	33 (14)	11 (5)	14 (10)	120 (37)	248 (75)	258 (64)	161 (46)	238 (59)
Total	63 (25)	27 (11)	34 (21)	159 (50)	251 (77)	259 (65)	162 (47)	248 (65)
First Occurrences								
African	15	8	10	26	0	0*	0	9
Eurasian	26	9	8	109	165	116	30	116
Total	41	17	18	135	165	116	30	125
Last Occurrences								
African	18	8	7	28	2	0	0	1
Eurasian	29	6	3	79	106	133	32	79
Total	47	14	10	107	108	133	32	80
Immigration								
Primary (Dispersal)	2	1	3	37	0	0*	0	7
Secondary (Origination)	24	8	6	81	0	0	0	2
Origination Rates								
African	0.08	0.10	0.19	0.15	0	0	0	0.20
Eurasian	0.13	0.17	0.22	0.21	0.11	0.09	0.07	0.11
Extirpation Rates								
African	0.10	0.10	0.13	0.16	0.11	0	0	0.02
Eurasian	0.14	0.11	0.08	0.15	0.07	0.11	0.08	0.08
Net Diversification Rates								
African	-0.02	0	0.06	-0.01	-0.11	0	0	0.18
Eurasian	-0.01	0.06	0.14	0.06	0.04	-0.02	-0.01	0.03

Unsurprisingly, the Chattian and Aquitanian stages exhibit low diversity on both landmasses (especially Africa), though this is almost certainly due to the paucity of sites of these ages, rather than a representation of their true biodiversity itself. Overall, generic diversity in Africa was vastly lower than that of Eurasia in all time intervals. These differences were especially pronounced prior to interchange, but remained considerable even after the influx of Eurasian immigrants in the Burdigalian. Family level data show a similar pattern, albeit by a lower numeric multiple. In Africa, Eurasian immigrants had already established themselves as significant components of the land mammal fauna before the GOWBI, representing between 41 and 52 percent of total genus diversity on the continent (Fig. 1A-B). In the Burdigalian, following the onset of interchange, this proportion swelled to 75 percent. African endemic genera did not decline immediately following the interchange, but their proportion of total diversity did, given the rapid increase in total diversity in the Burdigalian.

By contrast, Eurasian total diversity remained surprisingly stable throughout all stages, with a notable dip in the Aquitanian presumed to be an artifact of low sampling. African immigrants represented a minuscule fraction of total diversity in Eurasia, ranging from one percent in the Rupelian to only four percent in the Burdigalian. Endemic Eurasian genera showed virtually no decline throughout this time, though some family level diversity was lost. Thus, effects of the GOWBI on the Eurasian fauna appear almost negligible. Summaries for genus and family level occurrence data are reported in Table 1.

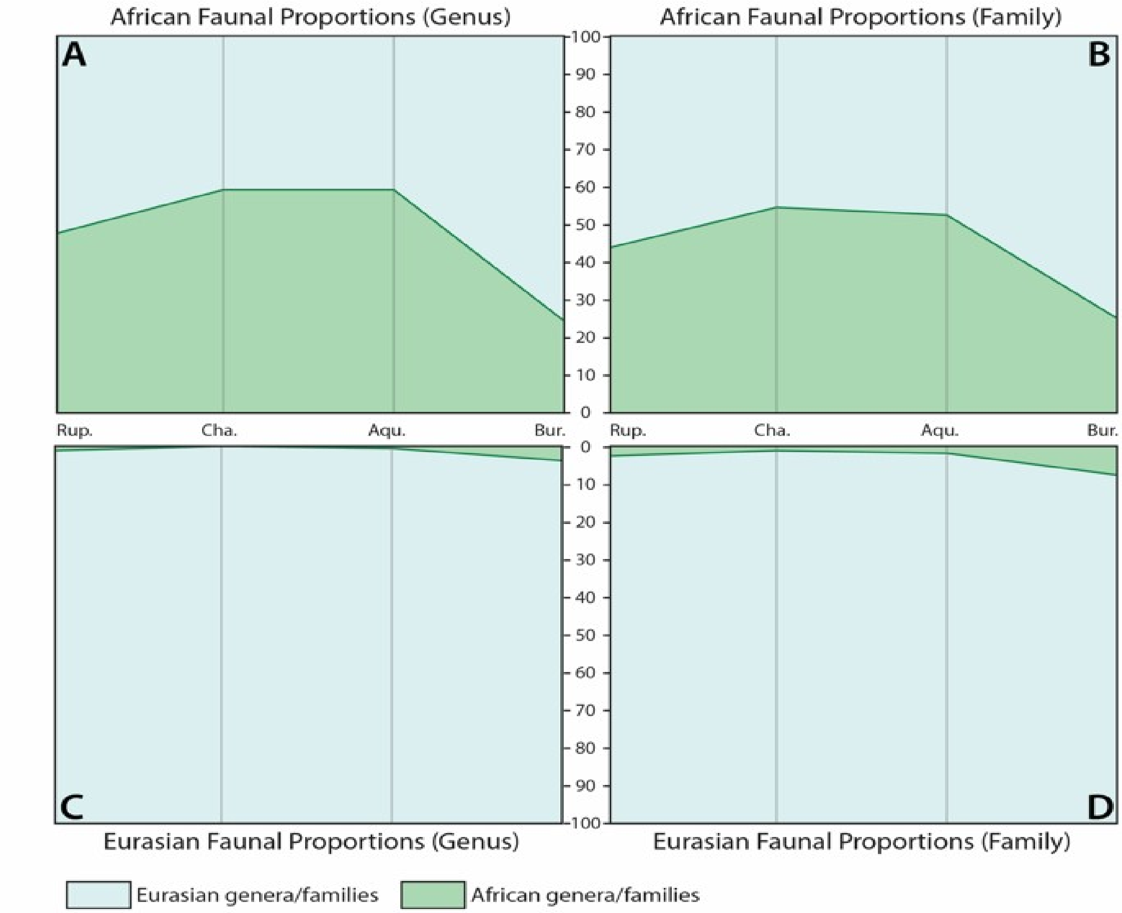

Figure 1. Graphs showing endemic and immigrant lineages as a proportion of total diversity through time. (A) Genus proportions in Africa; (B) Family proportions in Africa; (C) Genus proportions in Eurasia; (D) Family proportions in Eurasia.

Dispersal, Origination, and Extinction Data - In total, at least 27 families are presumed to have participated in the GOWBI via a dispersal sometime in the early Miocene (Table 2). A small number of these clades likely dispersed prior to the complete closure of a terrestrial landbridge, including at least one pedetid, viverrid, and tragulid (all southern migrants). Of the 27 total familial participants, 23 of these were Eurasian clades invading Africa, while only four African families managed to do the opposite. These families are composed of at least 81 total genera participants, including 72 Eurasian genera, and nine African. Hence, dispersal during, and immediately prior, to the GOWBI heavily favored clades of Eurasian origin over their endemic African counterparts.

Table 2. List of early Miocene immigrant families which participated in the GOWBI. The number of genera per family are listed, along with the number of inferred dispersal events within each group. References used for phylogenetic inferences are also listed, where applicable.

	Number of Genera	Dispersal Events	Phylogenetic Reference
African Primary Immigrants			
Amphicyonidae	3	2	
Anthracotheriidae	6	2	Rowan et al., 2015
Barbourofelidae	4	3	Wang et al., 2020
Bovidae	3	2	Mennecart et al., 2021
Chalicotheriidae	1	1	
Ctenodactylidae	2	1	López-Antoñanzas et al., 2016
Erinaceidae	3	3	
Felidae	5	1	
Giraffidae	2	2	Rios et al., 2017
Herpestidae	4	2	Morales et al., 2019
Muridae	2	1	
Mustelidae	3	1	
Ochotonidae	2	1	
Pedetidae	2	1	
Pseudocricetodontidae	1	1	
Rhinocerotidae	6	3	Geraads and Zouhri, 2021
Sanitheriidae	1	1	
Sciuridae	1	1	
Spalacidae	1	1	López-Antoñanzas et al., 2013
Suidae	6	3	Orliac et al., 2010
Tragulidae	2	2	Sanchez et al., 2015
Ursidae	1	1	
Viverridae	7	3	
Uknown Artiodactyl	4	3	Sanchez et al., 2015
Eurasian Primary Immigrants			
Deinotheriidae	2	2	
Gomphotheriidae	3	2	Wang et al., 2015
Hyainailouridae	2	1	
Mammutidae	2	2	Zhang and Wang, 2021

First occurrences in Africa saw a dramatic spike during the GOWBI, with at least 37 lineages of Eurasian genera dispersing into Africa in the Burdigalian, combined with the continued *in situ* evolution of earlier Eurasian migrants, as well as endemic African lineages. Even in the Rupelian, well before the onset of interchange, Eurasian immigrants experienced more first occurrences than African natives, owing primarily to the radiation of rodents and primates recorded in early Oligocene African faunas. In Eurasia, first occurrences prior to the GOWBI are due entirely to the *in situ* evolution of endemic genera. Only in the Burdigalian do identifiable African immigrants begin to arrive, and even then in comparatively small numbers. Nine African immigrants are recorded in the Burdigalian of Eurasia, with seven distinct dispersals and two subsequent originations.

Rates of evolution reveal that African natives experienced accelerated diversification in the early Miocene, though they were outpaced by the diversification of Eurasian immigrants in every time zone (Table 1). Between endemic faunas, Africa consistently experienced higher rates of origination and extirpation, implying higher volatility and turnover throughout the time interval. Extirpation rates among African endemics increased sequentially through time, while those for Eurasian immigrants remained relatively consistent pre and post-interchange. Net diversification rates on the African continent reveal an interesting contrast as well: endemic African genera averaged close to 0 net diversification (but very slightly positive; less than 0.01) across all four geologic stages, while Eurasian migrants averaged 0.06. Meanwhile, Eurasian natives experienced no observable increase in extirpation, or decrease in origination during the Burdigalian. Net diversification rates similarly suggest almost no overall change for endemic Eurasian mammals, while African migrants in Eurasia experienced a large positive spike in the

Burdigalian only. Eurasian natives also experienced a small, but slightly positive average net diversification rate through time (similar to African natives), but considerably lower than those that managed to establish themselves in Africa. These results suggest that, in terms of generic rates of evolution, the single biggest contributor to asymmetry in the GOWBI was the accelerated diversification of Eurasian migrants in Africa.

Rarefaction - Results of the rarefaction analysis are shown in Figure 2. Most notably, they reveal stark contrasts in total diversity and sampling extent between Africa and Eurasia, as well as among time intervals. The Burdigalian of Africa is well represented, particularly among Eurasian immigrants (Fig. 2A). The Rupelian appears reasonably well-sampled as well, with modestly flat curves observable in both endemic and immigrant lineages. The Chattian and Aquitanian stages in Africa are poorly represented, however, with short, predominantly vertical curves. In Eurasia, sampling and diversity appear far more consistent throughout time intervals, but the poor representation of African immigrants is obvious (Fig. 2B). The Aquitanian curve for Eurasian natives appears to have the steepest slope, suggesting that the decline in diversity shown in Table 1 may be an artifact of sampling. Overall, curves from both graphs show similarities in shape, though the extent to which particular faunas are represented through time varies significantly.

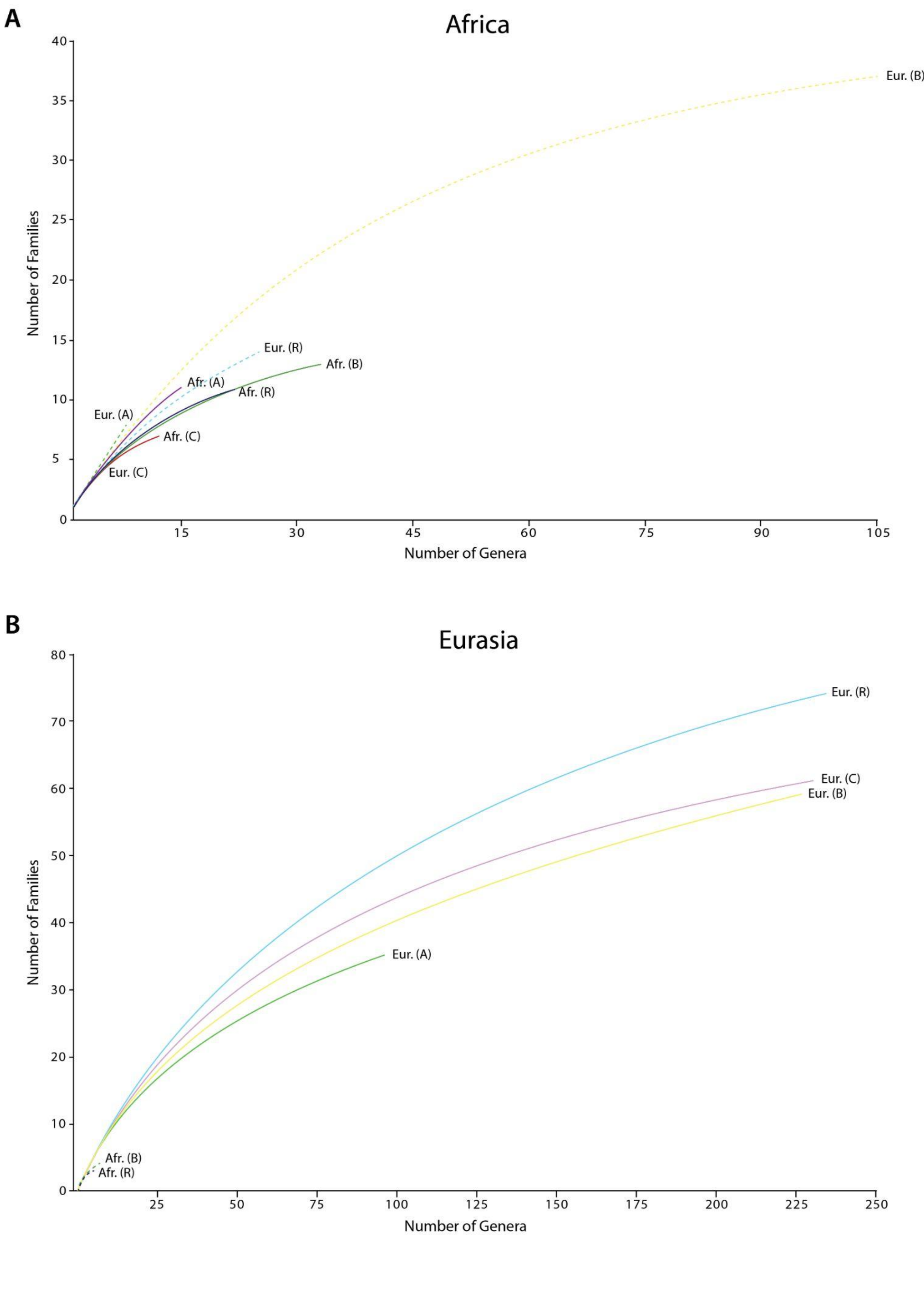
A
Africa
Number of Families
Number of Genera
0
5
10
15
20
25
30
35
40
15
30
45
60
75
90
105
Eur. (B)
Eur. (R)
Afr. (B)
Afr. (A)
Afr. (R)
Eur. (A)
Afr. (C)
Eur. (C)
B
Eurasia
Number of Families
Number of Genera
0
10
20
30
40
50
60
70
80
25
50
75
100
125
150
175
200
225
250
Eur. (R)
Eur. (C)
Eur. (B)
Eur. (A)
Afr. (B)
Afr. (R)

Figure 2. Rarefaction graphs of the African (A) and Eurasian (B) faunas in the late Paleogene and early Neogene. Abbreviations are: Afr = African; Eur = Eurasian; R = Rupelian; C = Chattian; A = Aquitanian; B = Burdigalian. Curves for native taxa are shown with solid lines, while immigrant taxa are denoted with dashed lines. Note that the scales are different for graphs A and B.

Discussion:

Numerous authors have recognized the dramatic upheaval of the insular mammal fauna in Africa in the early Miocene (e.g., Leakey et al., 2011; Cote et al., 2018; Rage and Gheerbrant, 2020). This event has also been examined in non-mammalian faunas as well (Harzhauser et al., 2007; Cossette et al., 2020; Georgialis et al., 2020). Coryndon and Savage (1973) were the first to quantify basic diversity data in Africa with respect to endemic and immigrant genera, while Gheerbrant and Rage (2006), Sen (2013), and Rage and Gheerbrant (2020) summarized Paleogene and Neogene dispersals into and out of Africa. The present study was the first to provide thorough quantitative measures of the GOWBI, using prior work on the GABI as a template (Marshall et al., 1982). It is also the first to examine dynamics of the GOWBI within the context of faunal biogeographic origin, rather than geographic location (i.e., previous work had considered all groups living in Africa in the Paleogene to be “endemic” African lineages, regardless of ordinal affinities and ancestral origins).

The results presented herein show low diversity in Africa at nearly all stages, with especially depauperate faunas in the Oligocene, prior to interchange. Historically, this was presumed to be an artifact of poor sampling of the African continent, although increasingly this is believed to reflect the true nature of African biodiversity (Rage and Gheerbrant, 2020). Indeed, recent work has suggested poor, or declining diversity in Africa in the Paleogene (Abbate et al., 2014; de Vries et al., 2021), although see Kappelman et al. (2003) and Sanders et al. (2004) for a counter-narrative. It should be noted, however, that arguments in favor of interchange. So, their success in the late Oligocene is not necessarily representative of African diversity more broadly. Thus, total diversity disparities between Africa and Eurasia prior to the GOWBI were likely high; much higher than those observed between North and South America during the GABI (Marshall et al., 1982). Given the large geographic size of Afro-Arabia, and apparently hospitable environmental conditions (e.g., Abbate et al., 2014; Kappelman et al., 2003), the landmass likely would have had vacant or under-utilized niches that primed immigrants for success upon arrival.

In comparing total diversity changes through time with the GABI, a similar pattern of replacement emerges between the two participant landmasses. In both cases, the northern landmass experienced relatively stable conditions, with a roughly 1:1 replacement of endemic lineages with southern migrants (Marshall et al., 1982). The southern landmass, by contrast, experienced a considerable boost to diversity following the arrival of northern immigrants. This increase is even more pronounced in the GOWBI, with a 152 percent increase in genera from the Rupelian to the Burdigalian, while South America experienced only a 64 percent increase through time. Among endemic faunas, South America experienced a gradual decline though successive ages, roughly corresponding to the gradual increase in North American migrants. Such a pattern is not observed in the GOWBI, however, as African natives do not decline in the Burdigalian, but rather diversify slightly.

Dispersal data here show an overwhelming bias in favor of Eurasian migrants. It should be noted, though, that the analysis conducted here does not represent the total north-south dispersals of taxa, but rather the dispersals of different groups of taxa depending on their geographic origin. Hence, it is possible that more families/genera migrated north during the

GOWBI than are reflected in Tables 1 and 2, but these would have been instances of Eurasian clades “re-migrating” back into Eurasia, and thus not particularly informative within the context of the present analysis. In comparison to the GABI, the GOWBI follows a nearly identical pattern of dispersal and subsequent origination. Not only do Laurasian landmasses send considerably more genera south than their Gondwana counterparts, the success of their respective immigrants differs starkly as well. Laurasian immigrants undergo approximately twice as many originations as they do dispersals, while Gondwanan migrants undergo comparatively little diversification. For instance, in the GOWBI, 109 first occurrences of Eurasian taxa in Africa include 37 separate dispersals, and 81 subsequent diversifications. The nine African first occurrences during the Burdigalian, by contrast, include seven dispersal events, and only two originations. Of these, seven of nine genera are proboscideans, which also comprise six out of seven dispersals, suggesting a strong taxonomic bias to northern immigration in the GOWBI (Table 2).

Results from origination rates are largely in agreement with those from the GABI as well. Endemic Gondwanan lineages experience a small increase in origination rates during interchange episodes, but these numbers are dwarfed by those of the Laurasian invaders. Meanwhile, Laurasian endemics experience virtually no net change to their rates as a result of interchange. Extirpation rates in the GOWBI show some divergence from the GABI, however. In the GABI, South American endemics undergo considerable increases in their extinction rates through time, and North American natives do too, albeit to a lesser extent. In the GOWBI, African endemics do experience a moderate increase in extirpation, but Eurasian natives do not. Thus, extinction/extirpation may have had a lesser role in the asymmetry of the GOWBI than it did in the GABI.

Among the most intriguing questions raised by the present analysis is, what contributed to the vast asymmetry of exchange between Africa and Eurasia? Decades of research on the GABI has attempted to offer solutions for such quandaries, with many hypotheses being put forth (e.g., Marshall et al., 1982; Vrba, 1992; Schultz et al., 1998; Prevosti et al., 2013; Amson et al., 2015; Carrillo et al., 2020). Among these explanations, competition, unrelated declines in endemic diversity, climate change, and vegetation/habitat change emerge as the most frequently cited. Proof of competition among immigrants and endemics in the GABI, however, has proven to be elusive, with the majority of recent authors rejecting this hypothesis (Prevosti et al., 2013; Carrillo et al., 2020; Croft et al., 2020). Abiotic factors, therefore, have been proposed as the most likely contributors to asymmetry in the GABI, given the open, dry savanna-like conditions that separated North America from South America (Woodburne et al., 2010). These regions likely acted as barriers to dispersal for South American taxa, which evolved under predominantly tropical conditions.

In the GOWBI, a similar story emerges. The global cooling regime that took hold in the late Eocene/early Oligocene likely stimulated a trend towards more open, arid habitats in Africa (Feakins and Demenocal, 2010; Lukens et al., 2017; Hall and Cote, 2021). This is in contrast to the predominantly dense, forested locales that dominated Africa in the Eocene, and fostered radiations of anthropoid primates (Jaeger et al., 2010). Numerous works have additionally shown that deteriorating climatic conditions in Africa likely contributed to habitat fragmentation in the Oligocene (Coster et al., 2015; Beard et al., 2016). Importantly, potential corridors of dispersal between Africa and Eurasia were also likely to be open, dry habitats in the late Oligocene/early Miocene, including the Bugti Hills region in Pakistan (Métais et al., 2017), and the “Levantine Corridor” of Israel (López-Antoñanzas et al., 2016; Grossman et al., 2019; Pandolfi et al., 2021). Taken together, these conditions suggest strong barriers to dispersal for African taxa, and likely also contributed to the increased volatility observed in origination and extirpation rates.

Biotic factors of asymmetry in the GOWBI are also questionable. Carnivores have frequently been examined as potential indicators of competition (Prevosti et al., 2013; Pires et al., 2017; Friscia et al., 2020), given their tight correlation with body size and feeding/predatory habits. In Africa, the endemic carnivore guild in the Paleogene was composed entirely of hyainailouroid hyaenodontans (Lewis and Morlo, 2010). By the middle Miocene, though, these endemic carnivores had disappeared entirely, and were replaced by members of the Carnivora (Friscia et al., 2020). It appears as though this replacement was not due to direct competition, however, given that there was little body-size overlap between native hyaenodontans and newly arrived carnivorans in the early Miocene (Borths and Stevens, 2017; Friscia et al., 2020). Even so, the replacement of archaic “creodonts” by carnivorans happened much faster in Africa than it did elsewhere (Friscia et al., 2020), leaving open at least some possibility that competition among immigrants and natives played a role in the turnover.

Conclusions:

This study examined the Great Old World Biotic Interchange using the quantitative template put forth for the Great American Biotic Interchange (Marshall et al., 1982). In doing so, it demonstrated that the GOWBI was an equally, if not more dramatic upheaval of the endemic African fauna than the GABI was for South America. Native African lineages declined rapidly as a proportion of total diversity, and experienced elevated volatility in origination and extirpation rates both before and after the onset of interchange. The relatively rapid influx of new Eurasian migrants into the continent contributed to a stark increase in total diversity in the Burdigalian. Eurasian mammal clades not only dispersed in large numbers into Africa, but evidently found favorable environmental and competitive conditions which permitted high rates of diversification. Meanwhile, the insular mammal clades of Africa managed to disperse in only very small numbers in the Burdigalian, and underwent very little subsequent diversification. These results suggest a pattern among large scale intercontinental exchange events, particularly those that involve diverse, cosmopolitan faunas engaging with isolated, highly endemic ones.

References

Abbate E, Bruni P, Ferretti MP, Delmer C, Laurenzi MA, Hagos M, Bedri O, Rook L, Sagri M, Libsekal Y. 2014. The East Africa Oligocene intertrappean beds: regional distribution, depositional environments and Afro/Arabian mammal dispersals. J. Afr. Earth Sci. 99: 463-489.

Amson E, Argot C, McDonald HG, de Muizon C. 2014. Osteology and Functional Morphology of the Forelimb of the Marine Sloth Thalassocnus (Mammalia, Tardigrada). J. Mamm. Evol., 22: 169-242.

Bacon CD, Silvestro D, Jaramillo C, Smith BT, Chakrabarty P, Antonelli A. 2015. Biological evidence supports an early and complex emergence of the Isthmus of Panama. PNAS 112: 6110-6115.

Beard KC. 2002. East of Eden at the Paleocene/Eocene boundary. Science 295: 2028-2029.

Beard KC, Coster PM, Salem MJ, Chaimanee Y, Jaeger J-J. 2016. A new species of Apidium (Anthropoidea, Parapithecidae) from the Sirt Basin, central Libya: first record of Oligocene primates from Libya. J. Hum. Evol. 90: 29-37.

Borths MR, Stevens NJ. 2017. The first hyaenodont from the late Oligocene Nsungwe Formation of Tanzania: Paleoecological insights into the Paleogene-Neogene carnivore transition. PloS One 12: e0185301-e0185301.

Carrillo JD, Faurby S, Silvestro D, Zizka A, Jaramillo C, Bacon CD, Antonelli A. 2020. Disproportionate extinction of South American mammals drove the asymmetry of the Great American Biotic Interchange. PNAS 117: 26281–26287.

Coryndon SC, Savage RJG. 1973. The origin and affinities of African mammal faunas. Special Papers in Paleontology. The Palaeontological Association, London 12: 121-135.

Cossette AP, Adams AJ, Drumheller SK, Nestler JH, Benefit BR, McCrossin ML, Manthi FK, Juma RN, Brochu CA. 2020. A new crocodylid from the middle Miocene of Kenya and the timing of crocodylian faunal change in the late Cenozoic of Africa. J. Paleo. 94: 1165-1179.

Coster PM, Beard KC, Salem MJ, Chaimanee Y, Brunet M, Jaeger JJ. 2015. A new early Oligocene mammal fauna from the Sirt Basin, central Libya: biostratigraphic and paleobiogeographic implications. J. Afr. Earth Sci. 104: 43-55.

Cote S, Kingston J, Deino A, Winkler A, Kityo R, MacLatchy L. 2018. Evidence for rapid faunal change in the early Miocene of East Africa based on revised biostratigraphic and radiometric dating of Bukwa, Uganda. J. Hum. Evol. 116: 95-107.

Croft DA, Gelfo JN, López GM. 2020. Splendid Innovation: The Extinct South American Native Ungulates. Ann. Rev. Ear. Plan. Sci. 48: 259-290.

Datta-Roy A, Karanth KP. 2009. The out-of-India hypothesis: what do molecules suggest? J. Biosci. 34: 687-697.

de Vries D, Heritage S, Borths MR, Sallam HM, Seiffert ER. 2021. Widespread loss of mammalian lineage and dietary diversity in the early Oligocene of Afro-Arabia. Comm. Biol. 4: 1172-1172.

Domingo L, Tomassini RL, Montalvo CI, Sanz-Perez D, Teresa Alberdi M. 2020. The Great American Biotic Interchange revisited: a new perspective from the stable isotope record of Argentine Pampas fossil mammals. Sci. Repo. 10: 1608-1608.

Ducrocq S, Boisserie J-R, Tiercelin J-J, Delmer C, Garcia G, Kyalo MF. Leakey MG, Marivaux L, Otero O, Peigné S, Tassy P, Lihoreau F. 2010. New Oligocene Vertebrate Localities from Northern Kenya (Turkana Basin). J. Vert. Paleo. 30: 293-299.

Feakins SJ, Demenocal PB. 2010. Global and African regional climate during the Cenozoic. In: Werdelin L, Sanders W (Eds.). Cenozoic Mammals of Africa. Berkeley, University of California Press, pp. 45-55.

Friscia AR, Macharwas M, Muteti S, Ndiritu F, Rasmussen DT. 2020. A Transitional Mammalian Carnivore Community from the Paleogene–Neogene Boundary in Northern Kenya. J. Vert. Paleo. 40: e1833895.

Foote M. 1994. Temporal variation in extinction risk and temporal scaling of extinction metrics. Paleobio. 20: 424-444.

Georgalis GL, Gawad MKA, Hassan SM, El-Barkooky AN, Hamdan MA. 2020. Oldest co-occurrence of Varanus and Python from Africa-first record of squamates from the early Miocene of Moghra Formation, Western Desert, Egypt. PeerJ (San Francisco, CA), 8: e9092–e9092.

Geraads D, Zouhri S. 2021. A new late Miocene elasmotheriine rhinoceros from Morocco. Acta Palaeontologica Polonica 66: 753-765.

Gheerbrant E. 2001. Histoire paléobiogéographique des mammifères paléogènes du domaine arabo-africain. H.D.R. thesis, Univ. Paris VI.

Gheerbrant E, Rage J-C. 2006. Paleobiogeography of Africa: How distinct from Gondwana and Laurasia? Palaeogeo., Palaeoclima., Palaeoeco. 241: 224-246.

Gottfried MD, Stevens NJ, Roberts EM, O'Connor PM, Chami R. 2009. A new Cretaceous lungfish from the Rukwa Rift Basin, Tanzania. Afr. Nat. Hist. 5: 31-36.

Graham A. 2018. The role of land bridges, ancient environments, and migrations in the assembly of the North American flora. J. Syst. Evol. 56: 405-29.

Granot R, Dyment J. 2015. The Cretaceous opening of the South Atlantic Ocean. Earth Plan. Sci. Lett. 414: 156-163.

Grossman A, Calvo R, López-Antoñanzas R, Knoll F, Hartman G, Rabinovich R. 2019. First Record of Sivameryx (Cetartiodactyla, Anthracotheriidae) from the Lower Miocene of Israel Highlights the Importance of the Levantine Corridor as a Dispersal Route Between Eurasia and Africa. J. Vert. Paleo. 39: e1599901.

Hall A, Cote S. 2021. Ruminant mesowear reveals consistently browse-dominated diets throughout the early and middle Miocene of eastern Africa. Palaeogeo. Palaeoclima. Palaeoeco. 567: 110253.

Hammer O, Harper DAT, Ryan PD. 2001. PAST: paleontological statistics software package for education and data analysis. Palaeontologia Electronica 4: 1-9.

Harzhauser M, Kroh A, Mandic O, Piller WE, Göhlich U, Reuter M, Berning B. 2007. Biogeographic responses to geodynamics: A key study all around the Oligo–Miocene Tethyan Seaway. Zoologischer Anzeiger, 246: 241-256.

Jaeger, J-J, Beard KC, Chaimanee Y, Salem M, Benammi M, Hlal O, Coster P, Bilal AA, Duringer P, Schuster M, Valentin X, Marandat B, Marivaux L, Métais E, Hammuda O, Brunet M. Late middle Eocene epoch of Libya yields earliest known radiation of African anthropoids. Nature 467: 1095-1098.

Kappelman J, Rasmussen DT, Sanders WJ, Feseha M, Bown T, Copeland P, Crabaugh J, Fleagle J, Glantz M, Gordon A, Jacobs B, Maga M, Muldoon K, Pan A, Pyne L, Richmond B, Ryan T, Seiffert E, Sen S, Todd L, Wiemann M, Winkler A. 2003. Oligocene mammals from Ethiopia and faunal exchange between Afro-Arabia and Eurasia. Nature 426: 549-552.

Leakey M, Grossman A, Gutiérrez M, Fleagle JG. 2011. Faunal Change in the Turkana Basin during the Late Oligocene and Miocene. Evol. Anth. 20: 238-253.

Lewis ME, Morlo M. 2010. Creodonta. In: Werdelin, L., Sanders, W. (Eds.), Cenozoic Mammals of Africa. Berkeley, University of California Press, pp. 543–560.

López-Antoñanzas R, Flynn LJ, Knoll F. 2013. A comprehensive phylogeny of extinct and extant Rhizomyinae (Rodentia): evidence for multiple intercontinental dispersals. Cladistics 29: 247-273.

López-Antoñanzas R, Gutkin V, Rabinovich R, Calvo R, Grossman A. 2016. A Transitional Gundi (Rodentia: Ctenodactylidae) from the Miocene of Israel. PLoS ONE 11: e0151804.

Lukens WE, Lehmann T, Peppe DJ, Fox DL, Driese SG, McNulty KP. 2017. The early Miocene critical zone at Karungu, western Kenya: an equatorial, open habitat with few primate remains. Front. Earth Sci. 5: 1-21.

Marshall LG, Webb SD, Sepkoski JJ Jr, Raup DM. 1982. Mammalian evolution and the Great American Interchange. Science. 215: 1351–1357.

Mennecart B, Métais G, Costeur L, Ginsburg L, Rössner GE. 2021. Reassessment of the enigmatic ruminant Miocene genus Amphimoschus Bourgeois, 1873 (Mammalia, Artiodactyla, Pecora). PLoS ONE 16: e0244661.

Métais G, Mennecart B, Roohi G. 2017. A new assemblage of stem pecoran ruminants from the Oligocene Chitarwata Formation, Bugti Hills, Baluchistan, Pakistan: Paleoenvironmental and paleobiogeographic implications. J. Asian Ear. Sci. 136: 40-49.

Morales J, Mayda S, Valenciano A, DeMiguel D, Kaya T. 2019. A new lophocyonid, Izmirictis cani gen. et sp. nov. (Carnivora: Mammalia), from the lower Miocene of Turkey. J. Syst. Palaeo. 17: 1347-1358.

Murphy WJ, Eizirik E, O'Brien SJ, Madsen O, Scally M, Douady CJ, Teeling E, Ryder OA, Stanhope MJ, de Jong WW, Spring MS. 2001. Resolution of the early placental mammal radiation using Bayesian phylogenetics. Science 294: 2348-2351.

O'Connor PM, Gottfried MD, Stevens NJ, Roberts EM, Ngasala S, Kapilima S, Chami R. 2006. A new vertebrate fauna from the Cretaceous Red Sandstone Group, Rukwa Rift Basin, southwestern Tanzania. J. Afr. Earth Sci. 44: 277-288.

Orliac MJ, Pierre-Olivier A, Ducrocq S. 2010. Phylogenetic relationships of the Suidae (Mammalia, Cetartiodactyla): new insights on the relationships within Suoidea. Zoologica Scripta: 39: 315-330.

The Paleobiology Database. (https://paleobiodb.org/).

Pandolfi L, Calvo R, Grossman A, Rabinovich R. 2021. Rhinocerotidae from the early Miocene of the Negev (Israel) and implications for the dispersal of early Neogene rhinoceroses. J. Paleo. 95: 1340-1351.

Pickford M. 1981. Preliminary Miocene mammalian biostratigraphy for Western Kenya. J. Hum. Evol. 10: 73-97.

Pires MM, Silvestro D, Quental TB. 2017. Interactions within and between clades shaped the diversification of terrestrial carnivores. Evolution 71: 1855-1864.

Prevosti FJ, Forasiepi A, Zimicz N. 2011. The Evolution of the Cenozoic Terrestrial Mammalian Predator Guild in South America: Competition or Replacement? J. Mamm. Evol. 20: 3-21.

Rage J-C, Gheerbrant E. 2020. Island Africa and Vertebrate Evolution: A Review of Data and Working Hypotheses. In Biological Consequences of Plate Tectonics. Springer International Publishing, pp. 251-264.

Rasmussen DT, Gutierrez M. 2009. A Mammalian Fauna from the Late Oligocene of Northwestern Kenya. Palaeontographica Abteilung 288: 1-52.

Ríos M, Sánchez IM, Morales J. 2017. A new giraffid (Mammalia, Ruminantia, Pecora) from the late Miocene of Spain, and the evolution of the sivathere-samothere lineage. PLoS ONE 12: e0185378.

Rögl F. 1999. Mediterranean and paratethys. Facts and hypotheses of an Oligocene to Miocene paleogeography. Geologica Carpathica 50: 330-349.

Rowan J, Adrian B, Grossman A. 2015. The First Skull of Sivameryx africanus (Anthracotheriidae, Bothriodontinae) from the Early Miocene of East Africa. J. Vert. Paleo. 35.

Sánchez IM, Quiralte V, Ríos M, Morales J, Pickford M. 2015. First African record of the Miocene Asian mouse-deer Siamotragulus (Mammalia, Ruminantia, Tragulidae): implications for the phylogeny and evolutionary history of the advanced selenodont tragulids. J. Syst. Palaeo. 13: 543-556.

Sanders WJ, Kappelman J, Rasmussen D. 2004. New large-bodied mammals from the late Oligocene site of Chilga, Ethiopia. Acta Palaeontologica Polonica 49: 365-392.

Sanders WJ, Miller ER. 2002. New proboscideans from the early Miocene of Wadi Moghara, Egypt. J. Vert. Paleo. 22: 388-404.

Schultz PH, Zarate M, Hames W, Camilión C, King J. 1998. A 3.3-Ma Impact in Argentina and Possible Consequences. Science 282: 2061-2063.

Seiffert ER. 2010. Chronology of Paleogene mammal localities. In: Werdelin L, Sanders W (Eds.). Cenozoic Mammals of Africa. Berkeley, University of California Press, pp. 19-26.

Sen S. 2013. Dispersal of African mammals in Eurasia during the Cenozoic: ways and whys. Geobios. 46: 159-172.

Simpson GG. 1980. Splendid isolation: the curious history of South American mammals. Yale University Press, New Haven, CT.

Stehli FG, Webb SD (eds). 1985. The Great American Biotic Interchange. Topics in Geobiology, Plenum Press, New York.

Stehlin HG. 1910. Remarques sur les faunules de Mammifères des couches Éocènes et Oligocènes du Bassin de Paris. Bulle. Soci. Geol. Fran. 9: 488-520.

Stigall AL. 2019. The invasion hierarchy: ecological and evolutionary consequences of invasions in the fossil record. Annu. Rev. Ecol. Evol. Syst. 50: 355-380.

Tabuce R, Marivaux L, Adaci M, Bensalah M, Hartenberger JL, Mahboubi M, Mebrouk F, Tafforeau P, Jaeger J-J. 2007. Early tertiary mammals from north Africa reinforce the molecular Afrotheria clade. Proc. Roy. Soc. Bio. Sci. Series B, 274: 1159-1166.

Van Couvering JA, Delson E. 2021. African Land Mammal Ages. J. Vert. Paleo. 40: e1803340.

Vermeij GJ. 1991. When biotas meet: understanding biotic interchange. Science, 253: 1099-1104.

Vrba ES. 1992. Mammals as a key to evolutionary theory. J. Mammal. 73: 1-28.

Wang S, Deng T, Tang T, Xie G, Zhang Y, Wang D. 2015. Evolution of Protanancus (Proboscidea, Mammalia) in East Asia. J. Vert. Paleo. 35: 1-13.

Wang X, White SC, Guan J. 2020. A new genus and species of sabretooth, Oriensmilus liupanensis (Barbourofelinae, Nimravidae, Carnivora), from the middle Miocene of China suggests barbourofelines are nimravids, not felids. J. Syst. Palaeo. 18: 783-803.

Webb SD. 1991. Ecogeography and the Great American Interchange. Paleobio. 17: 266-280.

Webb SD. 2006. The Great American Biotic Interchange: patterns and processes. Ann. Mo. Bot. Gard. 93: 245–257.

Werdelin L. 2010. Chronology of Neogene mammal localities. In: Werdelin L, Sanders W (Eds.). Cenozoic Mammals of Africa. Berkeley, University of California Press, pp. 27-43.

Werdelin L, Sanders WJ (eds). 2010. Cenozoic mammals of Africa. Berkeley, University of California Press.

Woodburne MO. 2010. The Great American Biotic Interchange: dispersals, tectonics, climate, sea level, and holding pens. J Mammal Evol, 17: 245.

Zhang X, Wang S. 2021. First report of Eozygodon (Mammutidae, Proboscidea) in Eurasia. Hist. Biol. 33: 1661-1670.